



저작자표시-비영리-변경금지 2.0 대한민국

이용자는 아래의 조건을 따르는 경우에 한하여 자유롭게

- 이 저작물을 복제, 배포, 전송, 전시, 공연 및 방송할 수 있습니다.

다음과 같은 조건을 따라야 합니다:



저작자표시. 귀하는 원저작자를 표시하여야 합니다.



비영리. 귀하는 이 저작물을 영리 목적으로 이용할 수 없습니다.



변경금지. 귀하는 이 저작물을 개작, 변형 또는 가공할 수 없습니다.

- 귀하는, 이 저작물의 재이용이나 배포의 경우, 이 저작물에 적용된 이용허락조건을 명확하게 나타내어야 합니다.
- 저작권자로부터 별도의 허가를 받으면 이러한 조건들은 적용되지 않습니다.

저작권법에 따른 이용자의 권리는 위의 내용에 의하여 영향을 받지 않습니다.

이것은 [이용허락규약\(Legal Code\)](#)을 이해하기 쉽게 요약한 것입니다.

[Disclaimer](#)

이학박사 학위논문

SK-BR-3 유방암 세포주에서
Lapatinib 내성 기전에 관한 연구

Mechanism of Lapatinib Resistance
in SK-BR-3 Breast Cancer Cells

2023년 2월

서울대학교 대학원

협동과정 중앙생물학 전공

김 소 현

SK-BR-3 유방암 세포주에서 Lapatinib 내성 기전에 관한 연구

지도 교수 임 석 아

이 논문을 이학박사 학위논문으로 제출함
2022년 10월

서울대학교 대학원
협동과정 중앙생물학 전공
김 소 현

김소현의 이학박사 학위논문을 인준함
2023년 1월

위 원 장 _____

부위원장 _____

위 원 _____

위 원 _____

위 원 _____

Mechanism of Lapatinib Resistance in SK-BR-3 Breast Cancer Cells

Directed by
Submitting a Ph.D. Dissertation of
Cancer Biology

October 2022

Interdisciplinary Graduate Program
of Cancer Biology
Seoul National University

Confirming the Ph.D. Dissertation written by
January 2023

Chair _____
Vice Chair _____
Examiner _____
Examiner _____
Examiner _____

Abstract

Mechanism of Lapatinib Resistance in SK–BR–3 Breast Cancer Cells

Human epithelial growth factor receptor 2 (HER2), a receptor tyrosine kinase, is considered as an important therapeutic target in breast cancer. Lapatinib is an effective tyrosine kinase inhibitor targeting EGFR and HER2 signal cascade. It has been approved for patients with HER2–positive metastatic breast cancer. Since majority of patients eventually acquire resistance, understanding the mechanism of lapatinib resistance remains a challenge.

In this study, lapatinib–resistant (LR) SK–BR–3 cells were established and characterized to understand the mechanism of resistance to lapatinib. LR cells showed an epithelial–to–mesenchymal transition (EMT) phenotype with expression of cancer stem cell markers and molecules associated with TGF– β , leading to increases of cell migration and invasion. On the other hand, RUNX3, a transcription factor well known as a tumor suppressor that could control cell migration and invasion

through regulation of molecules associated with EMT, was down-regulated in LR cells.

Replication stress was increased in LR cells. DNA damage repair capacity was enhanced and DNA damage response (DDR) mediated molecules were up-regulated in LR cells. Replication stress induced activation of DDR pathway and attenuated cytotoxicity of lapatinib in HER2-positive breast cancer cell lines. Collectively, these data suggest that activation of DDR pathway caused by replication stress contributes to resistance to lapatinib.

Keywords: HER2, Lapatinib, Resistance, EMT, Replication stress, DNA damage response

Student Number: 2017-31271

TABLE OF CONTENTS

ABSTRACT	i
TABLE OF CONTENTS	iii
LIST OF TABLES.....	iv
LIST OF FIGURES.....	v
INTRODUCTION	1
MATERIALS AND METHODS	6
I. Acquired resistance to lapatinib and epithelial-to-mesenchymal transition caused by downregulation of RUNX3.....	20
RESULTS	21
DISCUSSION	46
II. Replication stress activates DNA damage response and contributes to lapatinib resistance in SK-BR-3 cells	51
RESULTS.....	52
DISCUSSION	77
REFERENCES.....	80
ABSTRACT IN KOREAN.....	85
ACKNOWLEDGEMENT	87

LIST OF TABLES

I. Acquired resistance to lapatinib and epithelial-to-mesenchymal transition caused by downregulation of RUNX3

TABLE 1. Primer sequences for relative quantitative PCR
..... 12

TABLE 2. Population of breast cancer stem-like cells 32

LIST OF FIGURES

I. Acquired resistance to lapatinib and epithelial-to-mesenchymal transition caused by downregulation of RUNX3

Figure 1. Establishment of lapatinib-resistant (LR) cells... 23

Figure 2. LR cells show enhanced proliferation and spindle-like phenotype 25

Figure 3. LR cells acquire EMT phenotype and stemness.... 29

Figure 4. RUNX3 was downregulated by promoter methylation in LR cells 35

Figure 5. Overexpression of RUNX3 suppresses cell migration and invasion..... 40

Figure 6. TGF- β /SMAD pathway contributes to EMT process and development of lapatinib resistance 43

Figure 7. A model illustrating EMT process mediated by TGF- β /SMAD pathway regulated via RUNX3 during acquired resistance to lapatinib 45

II. Replication stress activates DNA damage response and contributes to lapatinib resistance in SK-BR-3 cells

Figure 8. High speed of fork progression in LR cells increases replication stress 54

Figure 9. CSC population shows enhanced replication stress in LR cells..... 59

Figure 10. Expression levels of homologous recombination repair (HR) mediated molecules are increased in LR cells... 64

Figure 11. DNA damage repair capacity is enhanced in LR cells..... 70

Figure 12. DDR activation induced replication stress affects lapatinib sensitivity 74

INTRODUCTION

Breast cancer is the most common malignancy in women. It is still one of the leading causes of tumor-related death in women worldwide. According to GLOBOCAN 2020, breast cancer ranked first in incidence (24.5 %) and tumor-related death (15.5 %) [1]. In Korea, the incidence rate of breast cancer is the highest among all cancers in women and the frequency of breast cancer occurrence has increased continuously [2]. Breast cancer is a very heterogeneous disease. It has four subtypes (luminal A, luminal B, HER2-positive, and triple-negative breast cancer (TNBC)) based on hormone receptors and human epidermal growth factor receptor 2 (HER2) status.

HER2, a transmembrane receptor tyrosine kinase (RTK) of HER family, consists of epidermal growth factor receptor (EGFR), HER2, HER3, and HER4. HER2 has no known natural ligand. It is activated by dimerization with other RTK members. Activated HER2 can regulate cell proliferation, survival, and migration through phosphatidylinositol 3-kinase (PI3K)/AKT and mitogen-activated protein kinase (MAPK) pathways [3, 4]. *HER2* is amplified in 20–25 % of breast cancer cases. And it is correlated with poor prognosis [5]. Thus, HER2 has been regarded as an important

therapeutic target in breast cancer and various HER2 targeted drugs have been developed.

Lapatinib, a small molecular tyrosine kinase inhibitor, can interrupt EGFR and HER2 signal cascade by binding to ATP-binding pockets of the HER2 intracellular domain [6]. It has been shown to be effective for treating advanced HER2-positive breast cancer and improving the prognosis of trastuzumab refractory patients when it is combined with capecitabine [7, 8]. However, a portion of these patients will lose response to lapatinib and eventually experience disease progression [5, 6]. Hence, exploring novel therapeutic strategies based on an understanding of the mechanisms involved in lapatinib resistance is needed.

Various mechanisms of lapatinib resistance have been reported. Several studies have suggested that resistance to HER2-targeted drugs including lapatinib is associated with epithelial-mesenchymal transition (EMT) [9, 10]. EMT is a process in which epithelial cells convert to spindle-shaped mesenchymal phenotype, lose cell-cell junction and cell polarity, and enable cell migration, invasion and generation of cancer stem cells [11-13]. EMT is triggered by various extracellular signals. TGF- β / suppressor of mothers against decapentaplegic (SMAD) is one of the important pathways that regulate EMT.

Human runt-related transcription factor 3 (RUNX3) is a transcription factor that can bind to DNA by interacting with CBF β /PEBP2 β , a cofactor [14]. Naturally, RUNX3 is localized in the nucleus where it functions as a tumor suppressor in various cancers including gastric, colon, and breast cancers. Correlated to these facts, RUNX3 is usually deleted, hypermethlylated, or mislocalized in most cancers, thereby losing its function as a tumor suppressor [14, 15]. In TGF- β /SMAD pathway, RUNX3 functions as an effector through interaction with C-terminal of SMAD [16, 17]. Several studies have demonstrated that overexpression of RUNX3 can inhibit EMT induced by TGF- β pathway [18] and that loss of RUNX3 can lead to enhanced EMT phenotype [19].

DNA replication is an important process for accurate cell division and maintenance of genome integrity. It is initiated at multiple genomic loci known as “replication origins” . Once replication origins are fired, replication forks will progress by replisome that can unwind the coiled DNA and synthesize new strands [20–22]. During this process, replication forks may encounter various obstacles such as depletion of dNTPs, replication and transcription conflicts, and secondary DNA structure that can cause replication stress. Replication stress refers to impediment of replication fork progression. It includes fork slowing down and collapsing. Since

replication stress can lead to DNA under-replication, abnormal mitosis, and hence genomic instability, S-phase checkpoint exists to repair and stabilize replication forks and inhibit cell cycle progression [20, 23, 24]. In brief, replication stress can induce single-strand DNA (ssDNA) and activate ATR-Chk1 pathway. Chk1 can suppress additional origin firing and delay S-phase progression until DNA replication is completed correctly. Simultaneously, DNA damage response (DDR) proteins can prevent replication fork degradation and restart stalled forks [21, 24, 25]. BRCA2 is known to be able to recruit RAD51 to stalled forks. RAD51 can protect the replication template from endonuclease. It can also restart fork through fork reversal [26, 27].

Activation of DDR is one of the well-known resistance mechanisms to chemotherapy, radiation, and targeted agents [28, 29]. Recent studies have reported that DDR activation is associated with resistance to HER2-targeted drugs. Up-regulation of PAPR1 contributes to tolerance of DNA damage induced by trastuzumab and activation of ATR-Chk1 pathway attenuates the antitumor effect of lapatinib [30, 31]. Clinical trials have shown that overexpressed excision repair cross-complementing group 1 (ERCC1) and X-ray repair cross complementing 1 (XRCC1) are associated with poor prognosis of HER2-positive breast cancer

patients who have received adjuvant trastuzumab [32]. Despite a correlation between DDR and HER2 targeted drug resistance, the specific function of DDR in lapatinib resistance is uncertain.

In this study, lapatinib-resistant cell lines from HER2-amplified SK-BR-3 human breast cancer cells were established. LR cells showed EMT phenotypes with TGF- β /SMAD pathway activated. TGF- β /SMAD signal pathway contributed to EMT process in parental cells. RUNX3 was involved in the mechanism of resistance to lapatinib by regulating EMT mediated by TGF- β /SMAD molecules.

Furthermore, replication stress was elevated and levels of stalled forks were increased in LR cells, especially in cancer stem-like cell population. Expression levels of HR key factors (including RAD51, RAD51 paralogs and XRCC3) and DNA damage repair capacity were increased in LR cells. Finally, replication stress activated DDR and attenuated cytotoxicity of lapatinib in HER2-positive breast cancer cell lines. These results provide further insight into the resistance mechanism of lapatinib. They could be used to help establish novel therapeutic strategies.

MATERIALS AND METHODS

1. Reagents

Lapatinib was kindly provided by GlaxoSmithKline (Brentford, UK) and AZD6738 was kindly provided by Astrazeneca (Cambridge, UK). Aphidicolin was purchased from Sigma Aldrich (St. Louis, MO, USA). These compounds were initially dissolved in dimethyl sulfoxide (DMSO) and stored at $-80\text{ }^{\circ}\text{C}$. Recombinant human TGF- β 1 was purchased from R&D systems Inc (Minneapolis, MN, USA). Compounds were reconstituted in sterile 4 mmol/L HCL containing 0.1% bovine serum albumin.

2. Cell lines and cell culture

A HER2 amplified human breast cancer cell line (SK-BR-3) was purchased from the American Culture Collection (ATCC; Manassas, VA, USA). T-47D, BT-549, and MDA-MB-453 cells were purchased from Korean Cell Line Bank (KCLB; Seoul, Republic of Korea). Cells were cultured in RPMI 1640 (Welgene; Gyeongsan-si, Republic of Korea) containing 10 % fetal bovine serum (Welgene) and 10 $\mu\text{g/mL}$ gentamicin (Thermo Fisher Scientific Inc.; Waltham, MA, USA) at $37\text{ }^{\circ}\text{C}$ in a 5 % CO_2 atmosphere.

3. Establishment of lapatinib-resistant SK-BR-3 cells

Lapatinib-resistant SK-BR-3 cells (LR cells) were established by continuously exposing cells to lapatinib, starting at a concentration of 30 nmol/L. The concentration was then gradually increased to 10 μ mol/L over seven months. Clonal selection was conducted using a serial dilution method. Lapatinib-resistant clones (LR#2 and LR#5) were then selected. Cells (pools of resistant cells) were expanded in RPMI-1640 medium containing 10% fetal bovine serum and 1 μ mol/L lapatinib.

4. Cell growth inhibitory assay

Cells ($0.8-6.5 \times 10^3$ in 100 μ L/well) were seeded into 96-well plates and incubated overnight at 37 °C in 5 % CO₂. These cells were exposed to increasing concentrations of lapatinib (dose range: 0-5 μ mol/L) for 3 days. After drug treatment, 50 μ L of 3-(4,5-dimethylthiazol-2-yl)-2,5-diphenyltetrazolium bromide solution (Sigma Aldrich) was added to each well and plates were incubated for 4 h at 37 °C. The medium was removed and formazan crystals were dissolved with 150 μ L of DMSO. The absorbance of each well was measured at 540 nm with a Thermo Scientific™

Multiskan™ GO Microplate Spectrophotometer (Thermo Fisher Scientific Inc.). Absorbance and IC₅₀ values of lapatinib were analyzed using Sigma Plot version 10.0 (Systat software, San Jose, CA, USA). Six replicate wells were included in each analysis and at least three independent experiments were conducted.

5. Cell proliferation assay

Cells (1×10^4) were seeded into 6-well plates and incubated at 37 °C overnight with 5 % CO₂. The number of cells was counted every 24 h for 5 days.

6. Cell cycle analysis

Cells were harvested, fixed in 75 % ethanol, and then stored at -20 °C for at least 48 h. After fixation, cells were treated with RNase A (Sigma Aldrich) at 37 °C for 2 h. These cells were stained with 20 µg/mL propidium iodide (Sigma Aldrich). Contents of DNA were measured with a fluorescence-activated Cell Sorting (FACS) Calibur flow cytometer (BD Biosciences). A total of 10,000 cells were analyzed for each experimental group.

7. Western blot analysis

Protein was extracted using RadioImmunoPrecipitation Assay (RIPA) buffer (50 mmol/L Tris-HCl (pH 7.5), 150 mmol/L NaCl, 1 % NP40, 0.1 % sodium dodecyl sulfate (SDS), 50 mmol/L NaF) containing protease inhibitors and phosphatase inhibitors. Equal amounts of proteins were separated on 8–12 % SDS–polyacrylamide gels. Resolved proteins were transferred onto nitrocellulose membranes. Blots were probed with primary antibodies overnight at 4°C. Antibody binding was detected using an enhanced chemiluminescence system (GE Healthcare life science; Chicago, IL, USA) according to the manufacturer's protocol.

8. Wound healing assay

Cells (4 or 10×10^5) were seeded into 6–well plates and incubated at 37 °C overnight with 5 % CO₂. Cells were scratched with sterile yellow tips and washed with PBS. Cells were incubated with medium. Images were captured and path length was measured using ImageJ program (National Institutes of Health (NIH); Bethesda, MD, USA).

9. Invasion assay

The invasive ability was evaluated using a Boyden chamber–

based cell invasion assay kit (Corning Inc; New York, USA). Cells were harvested and resuspended in serum free medium. Then 5×10^4 cells were seeded into the upper 24-well chamber. Medium with 20 % FBS or TGF- β 1 (5ng/mL) was added to the lower chamber as a chemoattractant. After 24 h, invaded cells were evaluated according to the manufacturer's instructions.

10. Spheroid formation assay

Resuspended single cells (2,000 or 10,000 cells/dish) were seeded into confocal dishes and incubated at 37 °C in 5 % CO₂ for 14 days. Spheroid formation was visualized with a Zeiss Laser Scanning Microscope (LSM) 800.

11. Cell surface molecule staining

Cells were harvested and resuspended with Brilliant stain buffer (BD Bioscience, San Jose, CA, USA). An antibody mixture of APC anti-human CD44 (BD Bioscience) and PerCP/Cyanine5.5 anti-human CD24 (BD Bioscience) was added and incubated in the dark for 30 min at 4 °C. Stained cells were analyzed using a fluorescence-activated Cell Sorting (FACS) Calibur flow cytometer (BD Biosciences).

12. mRNA extraction, RT-PCR, and relative quantitative PCR

RNA was extracted using Trizol reagent (Molecular research center Inc.; Cincinnati, OH, USA) or RNeasy Mini kit (Qiagen; Hilden, Germany) according to the manufacturer's instructions. Then 6 μ g of total RNA was used for cDNA synthesis with random hexamers (Bioneer; Daejeon, Republic of Korea). RNA expression levels were analyzed with an IQTM5 Optical Module (Bio-rad, CA, USA). Relative qPCR was done with a denaturation step at 95 °C for 5 minutes, followed by 40 cycles of denaturation at 95 °C for 1 minutes, primer annealing at 60 °C for 20 seconds, and primer extension at 72 °C for 30 seconds. A final extension at 72 °C for 5 minutes was then added. Samples were stored at 4 °C. RNA expression level was normalized against actin. Primer sequences are described in Table 1.

Table 1. Primer sequences used for relative quantitative PCR

Target	Sense (5'–3')	Antisense (3'–5')
SRC	CAGTGTCTGACTTCGACAACGC	CCATCGGCCTGTTTGGAGTA
SMAD2	CCGACACACCGAGATCCTAAC	AGGAGGTGGCGTTTCTGGAAT
SMAD3	CATCGAGCCCCAGAGCAATA	GTGGTTCATCTGGTGGTCACT
SMAD4	CCAATCATCCTGCTCCTGAGT	CCAGAAGGGTCCACGTATCC
SMAD7	GAATCTTACGGGAAGATCAACCC	CGCAGAGTCGGCTAAGGTG
SOX2	TACAGCATGTCTACTCGCAG	GAGGAAGAGGTAACCACAGGG
TGF- β 1	CCCTGGACACCAACTATTGC	TGCGGAAGTCAATGTACAGC
SNAIL	ACCACTATGCCGCGCTCTT	GGTCGTAGGGCTGCTGGAA
VIMENTIN	CCCTCACCTGTGAAGTGGAT	GCTTCAACGGCAAAGTTCTC
RUNX3	CAGAAGCTGGAGGACCAGAC	GTCGGAGAATGGGTTTCAGTT
ACTIN	AGA GCT ACG AGC TGC CTG AC	GGA TGC CAC AGG ACT CCA

13. Transcriptome data analysis

RNA was randomly fragmented for sequencing and reverse-transcribed into cDNA. Different adapters were attached to both ends of the prepared cDNA fragment by ligation. cDNA fragments were amplified with PCR. Sequencing service was provided by Macrogen Inc. (Seoul, Republic of Korea). Raw reads obtained from sequencing were then subjected to quality control analysis. Sequences were then mapped to the reference genome using the HISAT2 (v2.05) program considering splicing. Reads were then aligned followed by transcript assembly using StringTie (v1.3.3b) program based on information of aligned reads with the reference. Expression levels were then calculated based on transcript quantification of each sample as a normalized value considering both transcript length and depth of coverage. Expression profile was extracted by performing within normalization using Fragments Per Kilobase of transcript per Million mapped reads (FPKM). Pathway analysis was performed using public database, REACTOME [33], and dbEMT 2.0 [34].

14. Methylation sequencing

Genomic DNA was extracted using a DNeasy purification kit

(Qiagen). DNA fragments were prepared using a SureSelect Methyl-Seq Library Prep Kit (Agilent; CA, USA) according to the manufacturer's guide. Genomic DNA was hybridized using SureSelect Methyl-Seq Kit reagents (Agilent) following the manufacturer's protocol. Hybrids were captured with Dynabeads MyOne streptavidin beads (Thermo Fisher Scientific Inc.) and then eluted. By bisulfate conversion, modified unmethylated C residues and di-tagged DNA were enriched in PCR, resulting in double-stranded DNA (dsDNA). These DNAs were then sequenced using a HiSeq platform (Illumina). Sequencing was done by MacroGen Inc. Raw sequence reads are filtered based on quality. Only uniquely mapped reads were selected to sort. Index sequences and PCR duplicates were removed with SAMBAMBA (v0.5.9). The methylation ratio of every single cytosine location within on-target region was extracted from mapping results using 'methlratio.py' script in BSMAP. Results of coverage profiles were calculated as a number of C/effective CT counts for each cytosine in CpG, CHH, and CHG. Each cytosine locus was annotated using table browser function of the UCSC genome browser.

15. Transfection

LR cells with *RUNX3* overexpression and parental cells with *RUNX3* knockdown were obtained by transfection. *RUNX3* human tagged ORF plasmid and pCMV6-AC-GFP vector were purchased from OriGene Technologies Inc. (Rockville, MD, USA). LR cells were seeded into a culture dish. After 24 h, cells were initially transfected with 15 µg *RUNX3* plasmid or vector plasmid using a TransIT®-BrCa Transfection Reagent (Mirus Bio; Madison, WI, USA) according to the manufacturer's instructions. siRNA specific for *RUNX3* was obtained from Genolution (Seoul, Republic of Korea). Parental cells were initially transfected with siRNA at a final concentration of 120 nmol/L using G-fectin (Genolution) according to the manufacturer's instructions. After 48 h of incubation, cells were re-transfected with siRNA at the same concentration. Thereafter, transfected cells were seeded and subjected to other analyses. The sequence of the *RUNX3* specific siRNA was 5' -UGACGAGAACUACUCCGCUUU-3' .

The sequence of control (non-specific) siRNA was 5' -AAUUCUCCGAACGUGUCACGUUU-3'

16. Immunofluorescence assay (IFA)

Cells were seeded onto poly-L-lysine (Sigma Aldrich)-coated

cover slips. After 48 h, cells were fixed with 3.7 % paraformaldehyde for 10 min, permeabilized with 1 % Triton X-100 for 10 min, and blocked with 2 % BSA/DPBS for 1 h 30 min. For detecting DNA:RNA hybrid, cells were fixed with cold-100 % methanol at - 20 °C for 10 min and blocked with 5 % BSA/0.5 % triton X-100/DBPS for 1 h 30 min. After blocking, cover slips were incubated with primary antibodies overnight at 4 °C. Antibodies against ACTIN (Sigma Aldrich), CHK1 (Santa Cruz), p-RPA S4/8 (BETHYL laboratories Inc. Waltham, MA, USA), SOX2 (Abcam, Cambridge, UK), γ -H2AX (Cell signaling), and DNA-RNA Hybrid, clone S9.6 (Millipore, Burlington, MA, USA) were used. These cover slips were washed with DPBS and incubated with appropriate fluorophore-conjugated secondary antibodies (Invitrogen) for 1 h at 37 °C in the dark. After washing steps, cells were counter stained with 500 nM 4',6-diamidino-2-phenylindole (DAPI) (Invitrogen). Cover slips were then mounted onto slides using Faramount aqueous mounting medium (Dako, Glostrup, Denmark). Images were acquired using a Zeiss laser scanning microscope (LSM) 800.

17. EdU incorporation assay

Cells were seeded onto poly-L-lysine coated cover slips and

incubated with 10 $\mu\text{mol/L}$ 5-Ethynyl-2'-deoxyuridine (EdU) for 2 h. EdU detection was performed using Click-iT™ Plus EdU Cell Proliferation Kit for Imaging and Alexa Fluor™ 594 dye Kit (Invitrogen, Carlsbad, CA, USA) according to the manufacturer's protocol.

18. Alkaline comet assay

Alkaline comet assays were conducted using a Trevigen Comet Assay kit (Trevigen, Gaithersburg, MD, USA) according to the manufacturer's instructions. SYBR green was detected using a Zeiss LSM 800 laser scanning microscope. Tail moment was measured with a Comet IV software (Instem, Philadelphia, PA, USA).

19. DNA fiber assay

DNA fiber assay was performed as previously described [21]. Briefly, cells were labelled with 25 $\mu\text{mol/L}$ CldU (Sigma-Aldrich) for 20 min. After washing, cells were labelled with 250 $\mu\text{mol/L}$ IdU (Sigma-Aldrich) for 20 min. These cells were immediately trypsinized and resuspended in ice-cold PBS at 5×10^5 cells/mL. Then 2.5 μL of the cell solution was mixed with 7.5 μL lysis

buffer [200 mM Tris-HCL (pH 7.5), 50 mmol/L EDTA (pH 8), 0.5 % SDS] on a silane prep slide glass (Sigma-Aldrich). After 8 min, slides were tilted at 30–45 ° and resulting DNA spreads were air-dried. DNA spreads were fixed in 3:1 methanol/acetic acid at –20 °C overnight. DNA fibers were denatured with 2.5 M HCL for 1 h, washed with PBS, and blocked with 3 % BSA in 0.1 % Tween 20 for 1h 30 min. Slides were incubated with rat monoclonal anti-BrdU antibodies recognizing CldU (Abcam, 1:50) and mouse monoclonal anti-BrdU antibodies recognizing IdU (BD bioscience, Franklin Lakes, NJ, USA, 1:250) for 2 h at 37 °C followed by washing with a stringent buffer [10 mmol/L Tris-HCL (pH7.5), 400 mmol/L NaCl, 0.2 % Tween 20, 0.2 % NP40] for 15 min. DNA fibers were treated with goat anti-rat AlexaFluor–555 and goat anti-mouse AlexaFluor–488 (Invitrogen, 1:100) for 1h at RT, allowed to air-dry, and mounted in Faramount aqueous mounting medium (Dako). DNA fiber images were acquired using a Stellaris5 confocal microscope and DNA fiber length were measured with LAS X software (Leica, Wetzlar, German).

20. BrdU assay

Cells were incubated with 10 μ mol/L bromodeoxyuridine (BrdU) for 1 h 30 min. These cells were then immediately collected and

fixed with 70 % ethanol for at least 24 h. BrdU assay was performed using an FITC BrdU Flow Kit (BD Biosciences). Cells were incubated with 10 μ mol/L bromodeoxyuridine (BrdU) for 1 h 30 min. These cells were then immediately collected and fixed with 70 % ethanol for at least 24 h. After DNA denaturation with 4 M HCl for 20 min, cells were neutralized with phosphate/citric acid. Cells were incubated with anti-BrdU (1:30) for 30 min at 37 °C and stained with 7-Aminoactinomycin D (7-AAD). The fluorescence was measured with a FACS Canto II flow cytometer (BD bioscience).

21. Statistical analysis

All statistical analyses were performed using SigmaPlot version 10.0 (Systat software). A two-sided Student's t-test was used when appropriate. Results are expressed as mean \pm standard deviation (S.D.) or standard error (S.E.). Statistical significance was considered when a *p*-value was less than 0.05. All experiments were conducted in duplicate or triplicate and repeated at least twice.

**PART I. Acquired resistance to lapatinib
and epithelial-to-mesenchymal transition
caused by downregulation of RUNX3**

RESULTS

1. Establishment and characterization of lapatinib-resistant SK-BR-3 (LR) cells

LR cells were established by continuously exposing SK-BR-3 cells to lapatinib for more than seven months. After resistant cells were established, two clones (LR #2, LR #5) were selected (Fig 1A). To confirm the establishment of resistant cells, cytotoxicity of lapatinib was confirmed by MTT assay. Parental cells had IC_{50} values of 0.09 $\mu\text{mol/L}$, whereas LR cells and LR clones (LR #2 and LR #5) were viable when they were treated with lapatinib at concentrations up to 5 $\mu\text{mol/L}$ of (Fig. 1B). This result indicated that LR cells acquired resistance. Previously, it was verified that LR cells and LR clones were derived from SK-BR-3 cell line by DNA fingerprinting and that expression levels of HER2, HER3, and AKT were downregulated in LR cells compared with those in parental cells (Fig. 1C) [35]. To investigate differences between parental and LR cells, cell growth and cell cycle progression were examined. At 48 h time point, LR cells and LR clones proliferated approximately 20-fold compared those at 0 h time point. However, parental cells proliferated just 2-fold until 96 h (Fig. 2A). In LR

and LR clones, G1 phase was decreased 20 % whereas S and G2 phases were increased approximately 10 % each compared with parental cells (Fig. 2B). Moreover, LR cells showed a spindle-like morphology (Fig. 2C). Taken together, these results indicate that cell proliferation and cell cycle progression are enhanced in LR cells and that LR cells have a spindle-like morphology.

A.

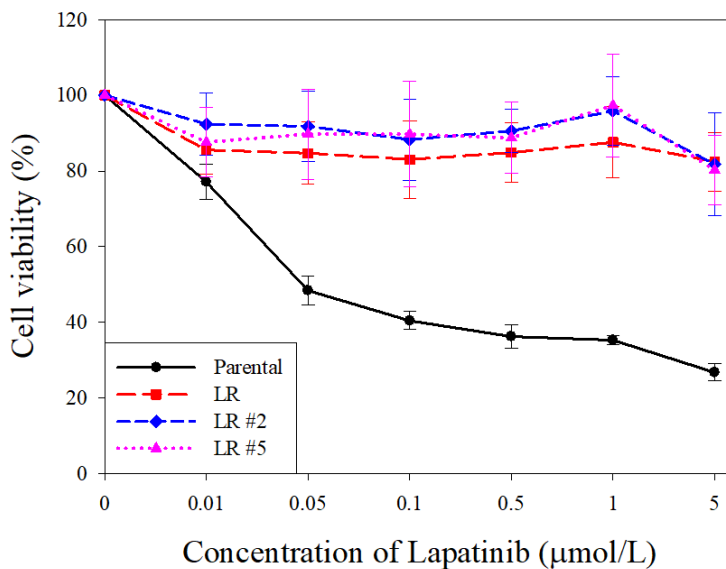
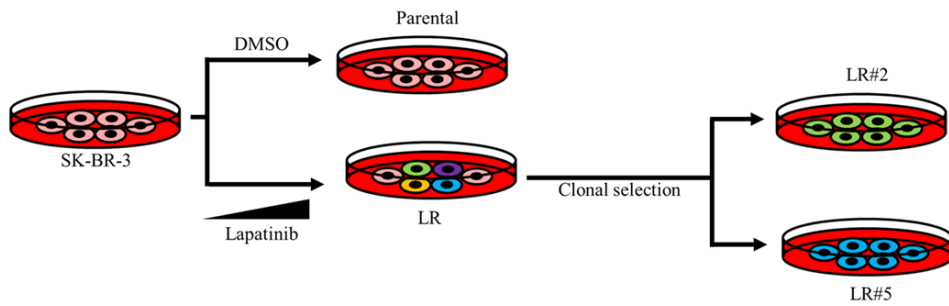


Figure 1. Establishment of lapatinib-resistant (LR) cells.

(A) Lapatinib-resistant cells were generated by culturing in increasing concentrations of lapatinib over 7 months. LR clones (LR#2 and LR#5) were generated by clonal selection using serial dilution method. (B) Cytotoxicity of lapatinib measured by MTT assay. Parental cells and LR cells were treated with lapatinib at indicated concentrations. After 72 h of treatment, cell viability was measured.

C.

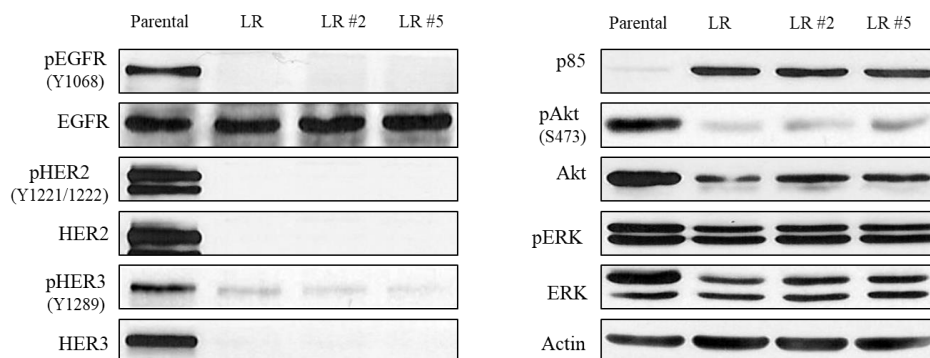


Figure 1. (C) Expression levels of HER2 signal transduction molecules detected by western blotting. Actin was used as a loading control.

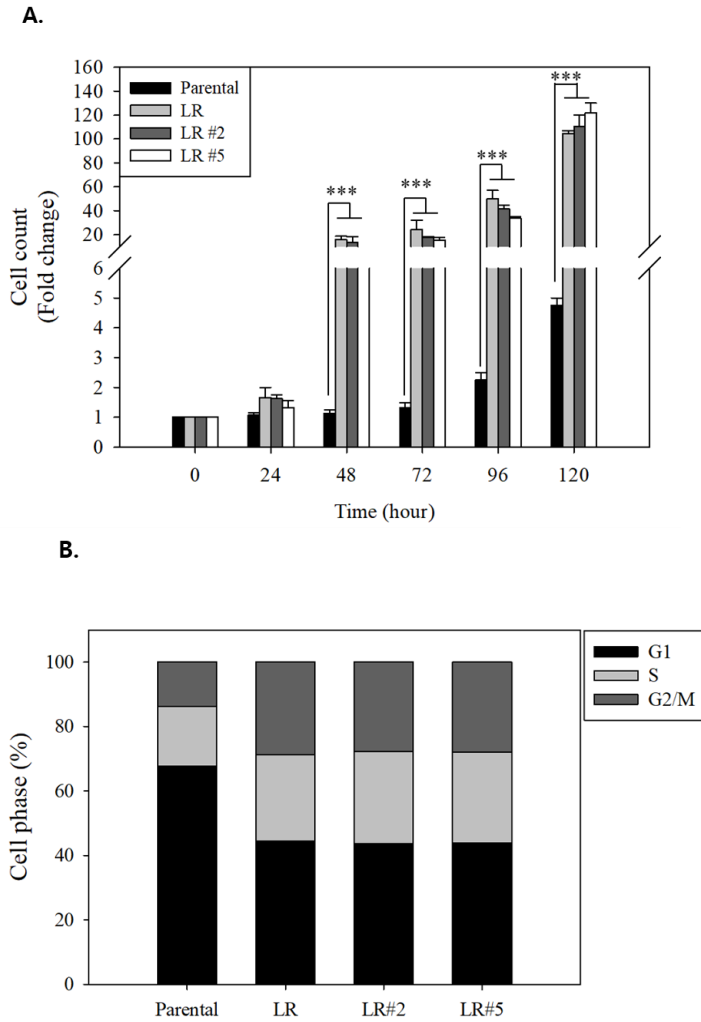


Figure 2. LR cells show enhanced proliferation and spindle-like phenotype. (A) Cell proliferation was measured every 24 h for 5 days (** $P < 0.001$). (B) Cell cycle progression was determined by measuring DNA contents using propidium iodide staining.

C.

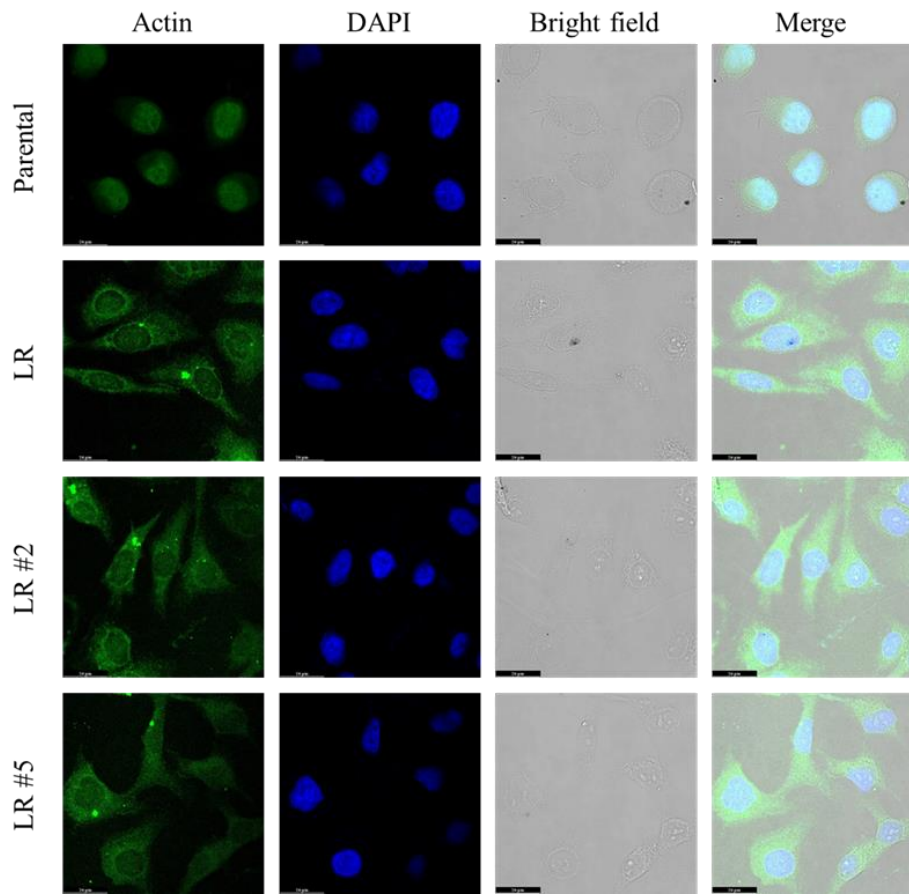


Figure 2. (C) Cells obtained at 63X magnification using confocal microscopy. Cytoplasm was stained with actin-antibody (Green) and nucleus was stained with DAPI (Blue). Scale bar, 10 μm .

2. LR cells show characteristic of epithelial to mesenchymal transition and cancer stem cells

Gaining spindle cell morphology and cancer stemness are well-known characteristics of EMT [12]. As LR cells showed spindle cell morphology (Fig. 2C), it was thought that parental cells underwent the EMT process and acquired resistance to lapatinib. Thus, expression levels of stem cell markers and EMT markers in LR cells were examined. mRNA expression levels of Src, Sox2, Nanog, Vimentin, and Snail were increased in LR cells (Fig. 3A). Correlated with mRNA expression, protein expression levels of these molecules were also increased. Moreover, expression levels of occludin-1 and claudin molecules known to be epithelial cell markers were decreased in LR cells (Fig. 3B). Next, cell migration and invasion abilities were evaluated. At 24 h time point, the relative ratio of wound closed was 4-fold higher in LR cells than in parental cells (Fig. 3C). In LR cells, wound was completely closed at 36 h to 48 h. However, in parental cells, wound was not completely closed until 120 h (Data not shown). Furthermore, the number of invaded cells was 2.5-fold higher in LR cells (Fig. 3D). Since expression levels of cancer stem cell markers were increased

in LR cells (Fig. 3A), to examine whether LR cells acquired stemness, spheroid formation assay was conducted. Parent cells grew in multiple layers without forming a spheroid. However, LR cells formed a spheroid (Fig. 3E). Cancer stem cell population (CD24⁻/CD44⁺) was significantly increased to 74.1±4.2% in LR cells (Fig. 3F and Table 3). These results suggested that LR cells acquired EMT phenotype and stemness.

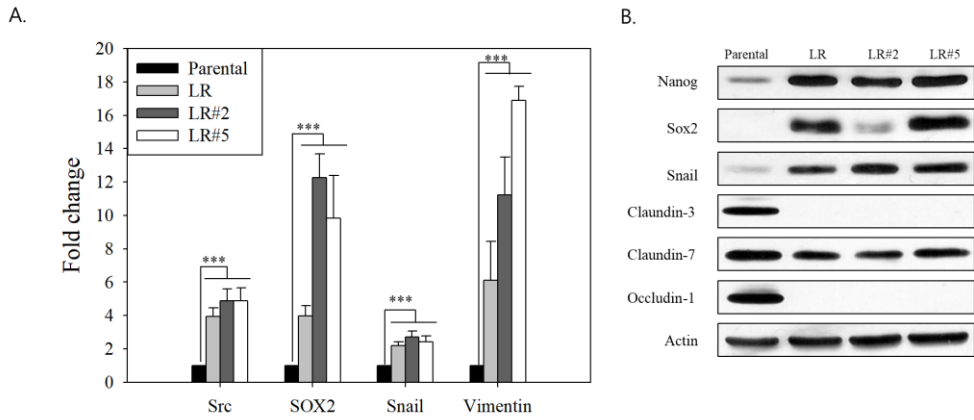


Figure 3. LR cells acquire EMT phenotype and stemness. (A) mRNA expression levels of EMT and CSCs markers in parental and LR cell lines. mRNA expression was detected by quantitative PCR. Actin was used as a control and mRNA expression was renormalized by the value of parental cells (** $P < 0.001$). (B) Protein expression levels of EMT, CSCs markers, and epithelial cell markers were detected by western blotting. Actin was used as a loading control.

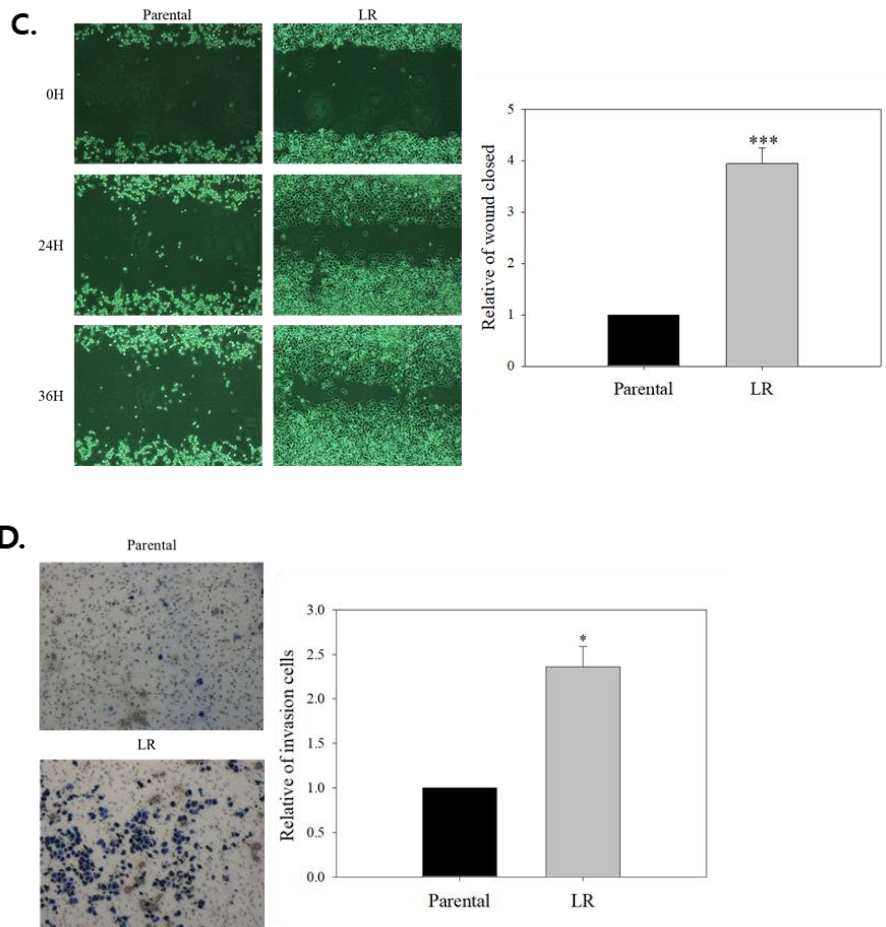


Figure 3. (C) Cell migration determined by wound healing assay. Images were obtained at 4X magnification. Relative wound closed was calculated from the average length of gap with 24 h time point data. Data are presented as mean \pm S.D. (***) $p < 0.001$ of three independent experiments. (D) Ability of cell invasion was determined by Boyden-chamber assay. Images were obtained at 4X magnification. Invasion cells were quantified. Data are presented as mean \pm S.D. (*) $p < 0.05$ of three independent experiments.

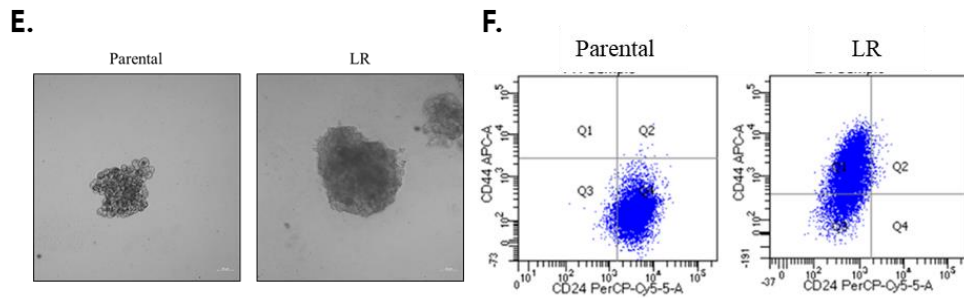


Figure 3. (E) Spheroid formation assay in parental and LR cells. Cells were cultured for 14 days and spheroid was visualized at 63X magnification. Scale bar indicates 10 μ m. (F) Expression levels of cancer stem cell surface markers were analyzed by flow cytometry. Dot plots represent expression patterns of CD24 and CD44. Cell subpopulations were defined by isotype controls.

Table 2. Population of breast cancer stem-like cells

Cell population \pm S.E. (%)		
	Parental	LR
CD24-/CD44-	2.5 ± 1.4	24.1 ± 3.35
CD24+/CD44-	96.2 ± 0.25	0.6 ± 0.6
CD24-/CD44+	0.0	74.1 ± 4.2
CD24+/CD44+	1.3 ± 1.2	1.3 ± 0.2

The table shows the percentage of subpopulation with \pm S.E. of three independent sorting experiments.

3. LR cells exhibit EMT phenotype via RUNX3 suppression

To identify molecules associated with EMT process in LR cells, transcriptome data were analyzed to identify differentially expressed genes (DEGs) between parental cells and LR cells. A total of 296 DEGs had $|\log_2$ ratio of fold change >2 and p -value <0.05 with functions in EMT regulation were identified [19]. DEGs were then subjected to reactome pathway analysis (Fig. 4A). As a result, interleukins and RUNX3 related pathways were enriched in DEGs (Fig. 4B). Because interleukins are known to be regulated by RUNX3, RUNX3 was chosen for further analysis. In LR cells, mRNA expression of RUNX3 was reduced by approximately 9-fold compared with that in parental cells (Fig. 4C). Its protein expression level was also decreased in LR cells compared with that in parental cells (Fig. 4D). Next, to determine RUNX3 down-regulation mechanism in LR cells, methylation sequencing was conducted. Average *RUNX3* promoter methylation ratio was significantly increased in LR cells (Fig. 4E). To confirm this result, 5-azacytidine was used for treatment and RUNX3 expression was examined. After 5-azacytidine treatment, RUNX3 mRNA level was

up-regulated in LR cells but not changed in parental cells (Fig. 4F). Correlated with mRNA analysis results, its protein expression level was also increased in LR cells but not changed in parental cells (Fig. 4G). BT-549 cells were used as a negative control and T-47D cells were used as a positive control [36]. These results indicated that RUNX3 was downregulated by promoter hypermethylation in LR cells.

A.

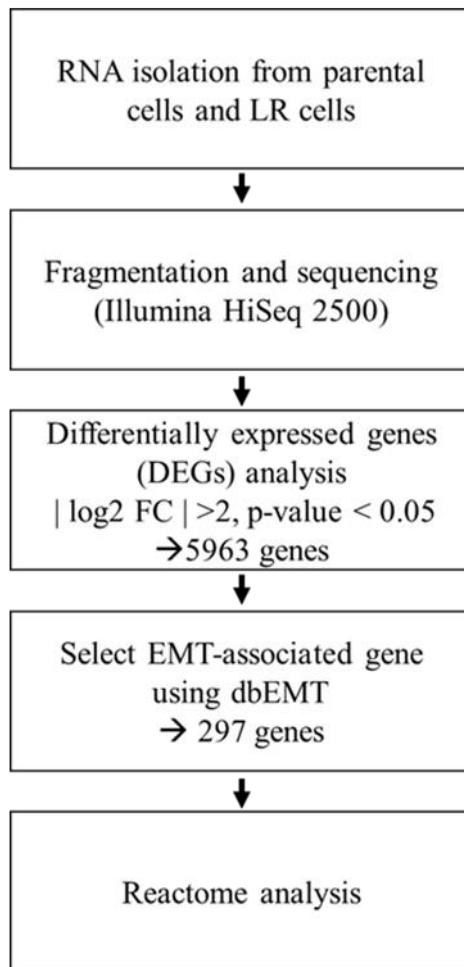


Figure 4. RUNX3 was downregulated by promoter methylation in LR cells. (A) Scheme of transcriptome analysis.

B.

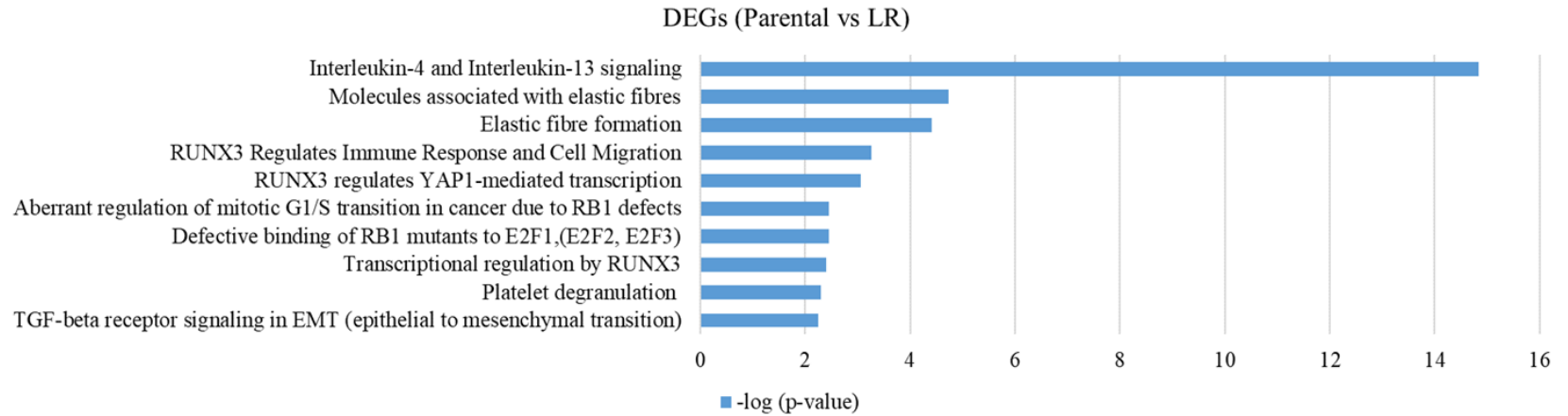


Figure 4. (B) Reactome pathway enrichment of RUNX3 and EMT associated DEGs.

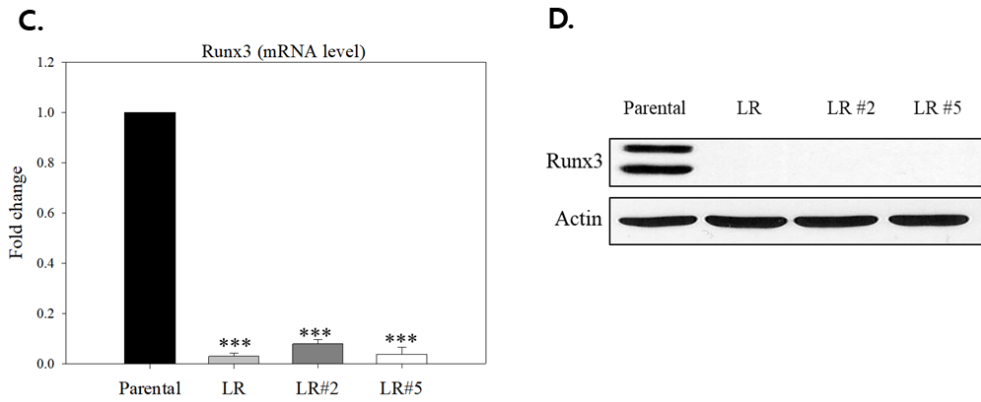


Figure 4. (C) mRNA level of RUNX3 was determined by quantitative real-time PCR. Actin was used as a control and mRNA expression was renormalized by the value in parental cells. Data are presented as mean \pm S.D. (***) $P < 0.001$) of three independent experiments.

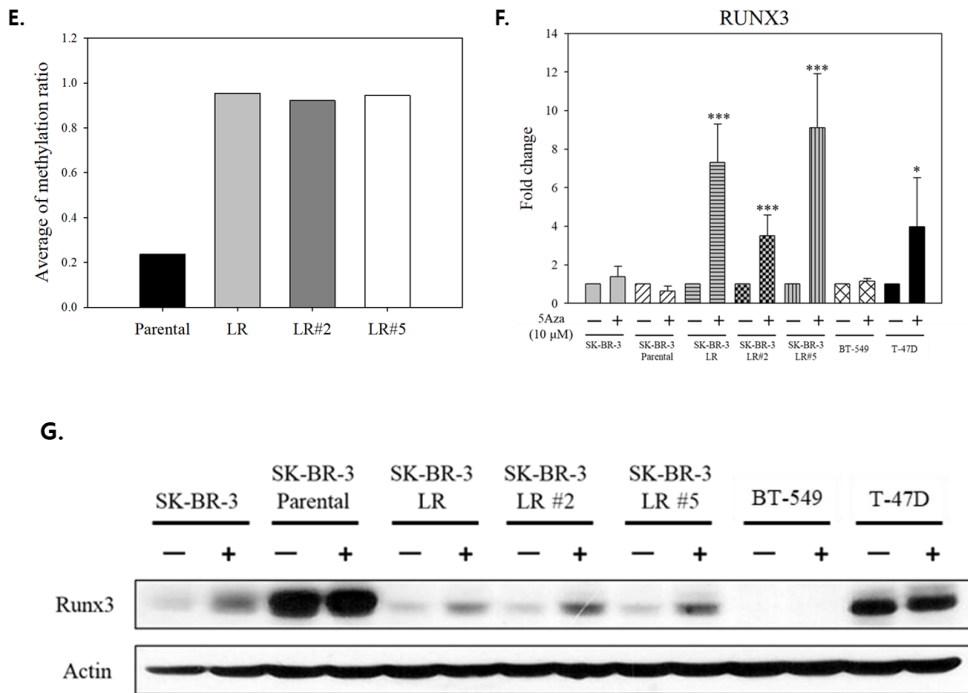


Figure 4. (E) Average methylation of *RUNX3* promoter calculated with methylation sequencing data. (F) Cells were treated with 5-azacytidine (5Aza, 10 μ M). After 72 h, cells were harvested and RNA was extracted. Relative mRNA expression of *RUNX3* was confirmed by quantitative real-time PCR. Fold change with respect to control was calculated using $\Delta\Delta$ Ct method. (G) Cells were treated with 5-azacytidine (5Aza, 10 μ M). After 72 h, cells were harvested and protein was extracted. Expression level of *RUNX3* protein was determined by western blotting.

4. RUNX3 suppresses EMT process

To confirm effects of RUNX3 on EMT in LR cells, RUNX3 overexpression cells were established (Fig. 5A) and their migration and invasion abilities were measured. The relative wound closure was decreased to 0.52 ± 0.06 in LR cells with overexpression of RUNX3 (Fig. 5B). Also, in LR cells with overexpression of RUNX3, relative invasion cells were significantly decreased to 0.18 ± 0.05 (Fig. 5C). These results suggested that EMT was suppressed by RUNX3.

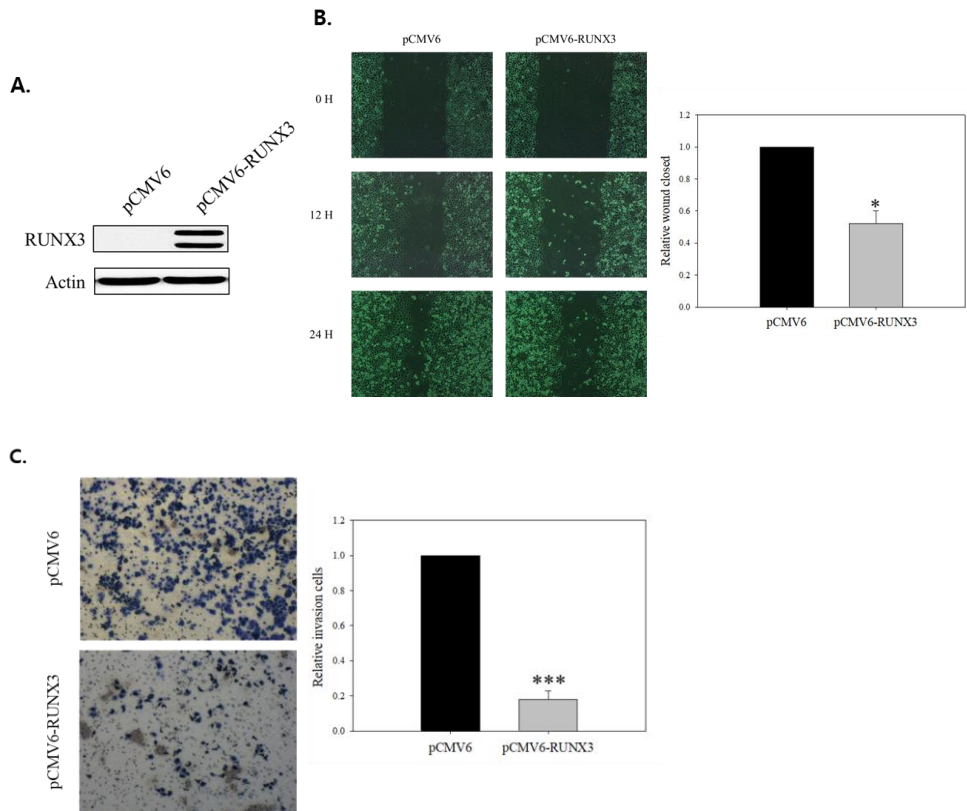


Figure 5. Overexpression of RUNX3 suppresses cell migration and invasion. (A) LR cells were transfected with vector plasmid (pCMV6) or *RUNX3* containing plasmid (pCMV6-*RUNX3*). Cells were selected with G418 for 72 h. RUNX3 expression was confirmed by western blotting. (B) Representative images (Magnification X4) of woundhealing assay and percentage of wound closed (* $p < 0.05$). pCMV6 indicates cells transfected with an empty-vector and pCMV6-*RUNX3* indicates cells transfected with RUNX3 for overexpression. (C) Representative images (magnification X4) of invasion cells and number of cells in a field (** $p < 0.005$).

5. TGF- β /SMAD signal pathway promotes EMT during acquisition of lapatinib resistance

RUNX3 as a transcription factor regulates multiple signal transduction molecules. Thus, specific signal pathways involved in EMT in LR cells were identified. Reactome pathway analysis showed that genes associated with TGF- β pathway were enriched (Fig. 6A). Transcriptome data for TGF- β core genes showed that activating TGF- β signal factors such as SMAD5, SMAD7, TGFBR2, and TGFBR3 were up-regulated in LR cells (Fig. 6A). Moreover, INHBB, an inhibitory molecule, was downregulated in LR cells (Fig. 6A). mRNA expression levels of TGF- β 1, SMAD3, SMAD4, and SMAD7 were significantly increased in LR cells based on quantitative PCR (Fig. 6B). Protein expression levels of SMAD3 and SMAD4 were also increased in LR cells (Fig. 6C). To confirm that TGF- β could induce EMT, TGF- β was used to treat parental cells. Expression of SMAIL and phosphorylation levels of SMAD3 and SRC were increased in cells treated with TGF- β (Fig. 6D). Moreover, cell invasion was increased to approximately 3-fold after TGF- β treatment (Fig. 6E). These results indicate that activation of TGF- β pathway can induce EMT that confers to

lapatinib resistance. Previous studies have demonstrated that RUNX3 is associated with TGF- β signaling in EMT [18, 19]. Thus, RUNX3 might regulate EMT through TGF- β pathway. To test this possibility, RUNX3 was knocked down using siRNA in parental SK-BR-3 cells. Cells with RUNX3 knockdown showed up-regulation of Src, SMAD2, SMAD3, SMAD4, TGF- β 1, Snail, and vimentin (Fig. 6F). These data suggest that downregulation of RUNX3 contributes to activation of TGF- β pathway and leads to EMT (Fig. 6G).

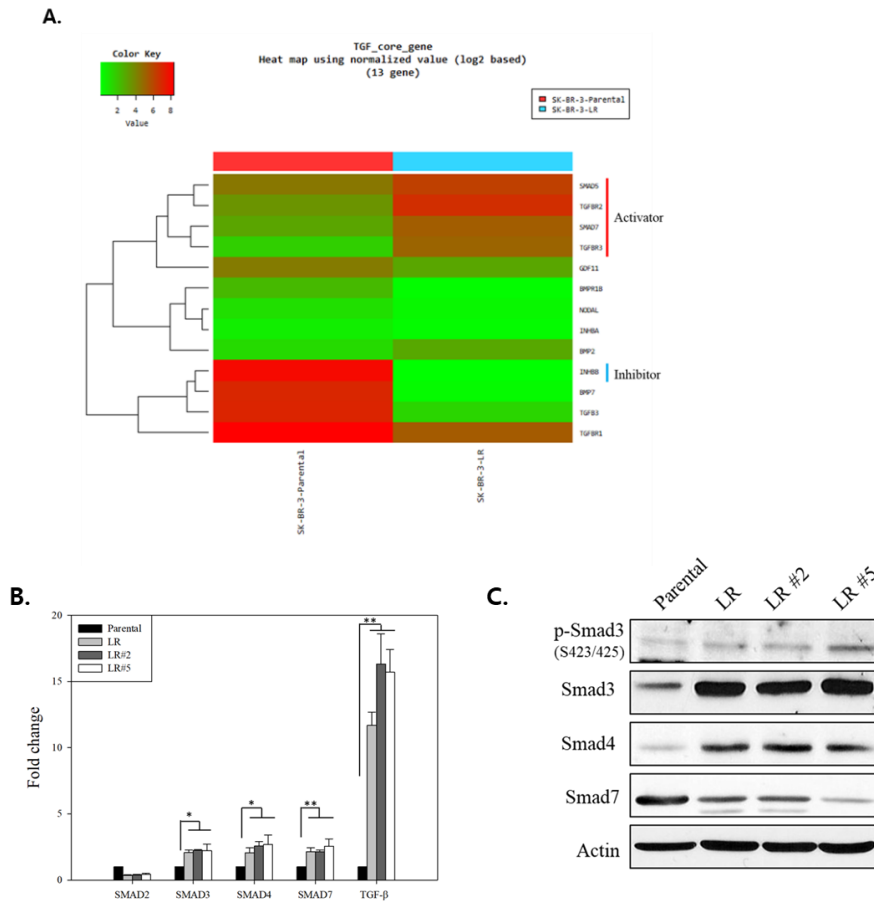


Figure 6. TGF- β /SMAD pathway contributes to EMT process and development of lapatinib resistance. (A) Expression levels of TGF- β /SMAD pathway core molecules were analyzed by RNA sequencing. (B) mRNA levels of TGF- β /SMAD molecules were determined by quantitative real time PCR. Actin was used as a loading control and mRNA expression was renormalized by the value in parental cells (* $P < 0.05$, ** $P < 0.005$) (C) Western blot analysis results for p-SMAD3 (S423/425), SMAD3, SMAD5, and SMAD7 are shown.

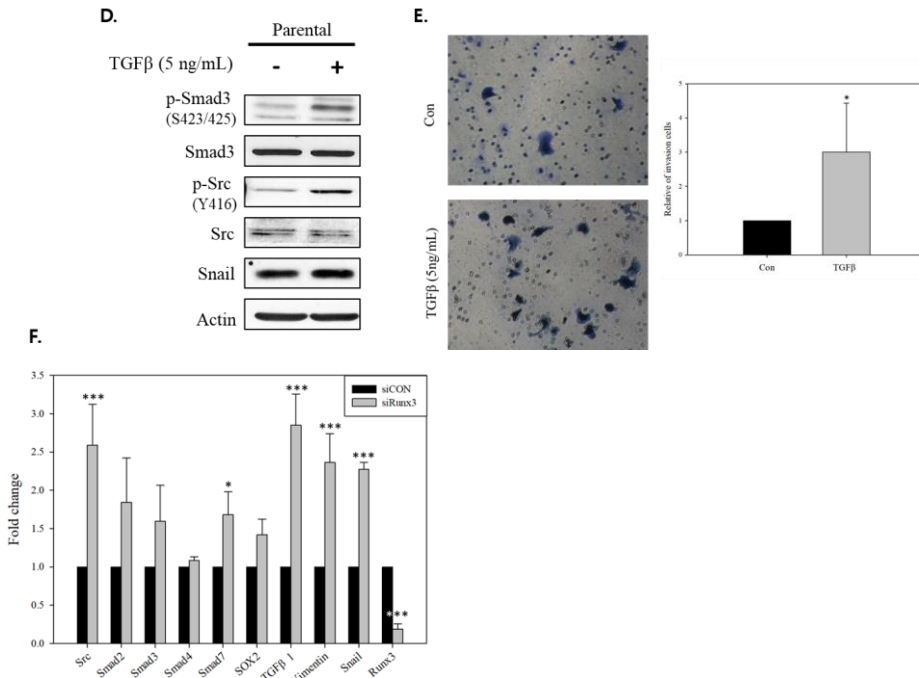


Figure 6. (D) Parental cells were treated with TGF- β at 5 ng/ml for 48 h. Whole-cell extracts were analyzed by western blot with antibodies recognizing phosphorylated and total SMAD3, SRC, SOX2 and SNAIL. (E) Parental cells were treated with TGF- β at 5 ng/ml. After 48 h, cell invasion was determined using Boyden chamber assay (Magnification: X10, *P<0.05). (F) Using siRNA knock-down system, RUNX3 was down-regulated in parental cells. mRNA levels of EMT markers and TGF- β pathway molecules were determined by quantitative real-time PCR. The fold change of RUNX3 in cells with RUNX3 knockdown compared to the control was calculated (*P<0.05, ***P<0.001).

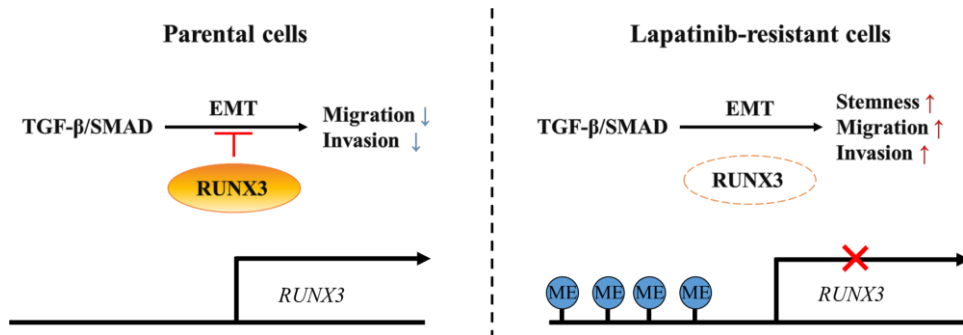


Figure 7. Model illustrating EMT process mediated by TGF- β /SMAD pathway regulated via RUNX3 during acquired resistance to lapatinib. In LR cells, RUNX3 was down-regulated by promoter methylation. Down-regulation of RUNX3 induced EMT was mediated by activation of TGF- β /SMAD signal transduction. LR cells then acquired EMT phenotype and cancer stemness.

DISCUSSION

Although lapatinib is a clinically-validated and approved drug for HER2-amplified breast cancer, acquired resistance is a critical problem. It is crucially necessary to understand the mechanism of resistance to overcome the resistance and to establish novel treatment strategies. Thus, mechanisms involved in acquired resistance to lapatinib in HER2-amplified breast cancer cell lines were investigated in this study.

The EMT process is one well-known mechanism of resistance to HER2-targeted drugs, including lapatinib. Previous studies have shown that up-regulation of EMT markers such as snail and vimentin can lead to EMT and confer trastuzumab or lapatinib resistance [9, 37]. Consistent with previous studies, LR cells exhibited characteristics of EMT, including spindle-like morphology, cell migration, and cell invasion. Expression levels of EMT markers such as Snail and Vimentin were also increased in LR cells. Collectively, this study provides evidence that EMT is associated with acquired resistance to lapatinib.

In a previous study, Src phosphorylation was significantly increased in LR cells [35]. Src is a non-tyrosine kinase that belongs to Src family kinases (SFKs). Src can interact with p120 catenin that can lead to loss of cell-cell junctions and facilitate cell

migration during EMT. Moreover, Src regulates expression of matrix metalloproteinases (MMPs) that are zinc-dependent endopeptidases, leading to degradation of extracellular matrix (ECM) [38]. A previous study has reported that Src is activated in lapatinib-resistant cell line and that src inhibitor can overcome resistance to lapatinib [39].

Although it is well known that EMT contributes resistance to lapatinib, specific mechanisms that regulate the EMT process remain unclear. It has been reported that epigenetic modification contributes to drug resistance [40]. Previous studies have also suggested that DNA methylation and transcriptional changes of EMT markers or tumor suppressor genes can lead to acquired resistance to cancer therapeutic agents in various cancers [40, 41]. In the present study, distinct differences in the expression of EMT markers between parental and LR cells were observed, although there were no differences in methylation of these EMT markers. On the contrary, RUNX3 was down-regulated in LR cells due to hypermethylation at promoter CpG islands.

RUNX3 is a transcription factor that functions as a tumor suppressor in various cancers. In gastric cancer, it is well-known that RUNX3 regulates EMT through multiple mechanisms. A previous study has reported RUNX3 knockdown gastric cancer cells

show loss of epithelial cell characteristic and gain mesenchymal cell characteristic by up-regulating Vimentin via regulation of microRNA. And gastric cancer cells with overexpression of RUNX3 show restored epithelial cell characteristics [42]. Consistent with these results, overexpression of Runx3 effectively suppressed cell migration and invasion of LR cells. In breast cancer, it is well-known that Runx3 functions as a tumor suppressor by mediating estrogen receptor degradation [15]. However, its functions as an EMT suppression factor and regulatory mechanism of EMT remain unclear. Thus, this study provides a useful in vitro model to understand the EMT suppressive role of RUNX3 in breast cancer.

Several studies have suggested that RUNX3 is associated with drug resistance. Previous studies have reported that loss of RUNX3 can lead to increased expression of multidrug resistance proteins (MRPs) and confer resistance to chemotherapeutic drugs [43, 44]. In the present study, there were no significant differences in the expression of MRPs between parental cells and LR cells lines (data not shown). However, RUNX3 is involved in resistance to lapatinib by modulating the EMT process. Therefore, this study is helpful for understanding drug resistance mechanisms associated with RUNX3.

Using reactome analysis, TGF- β associated genes were significantly different between parental cells and LR cells. TGF-

β /SMAD pathway is an important pathway for EMT regulation. Mutations in TGF- β and SMAD molecules can induce disease progression in gastrointestinal, colon, and pancreatic cancers. In breast cancer, a point mutation (S387Y) in *TGFBR1* is associated with the progression of breast cancer [45]. Therefore, mutations in TGF- β /SMAD pathway associated molecules were analyzed using whole exome sequencing data. However, pathogenic mutations were not detected in parental or LR cells.

A previous have reported that EGFR/HER2 heterodimer can induce AKT dependent EMT process through phosphorylation of SMAD3 at Ser208. Consist with this result, inhibition of EGFR/HER2 signaling suppressed EMT by attenuating AKT dependent TGF- β /SMAD pathway [46]. However, in the present study, AKT was decreased in LR cells (Fig. 1B) and TGF- β pathway was activated through phosphorylation of SMAD3 at S423/425 independent with AKT. These results indicate that AKT pathway independent molecules can modulate TGF- β pathway in lapatinib-resistant models used in the present study. Previous studies have confirmed that *RUNX3*-null gastric epithelial cell lines were sensitized to TGF- β 1 to undergo EMT [19]. A recent study has also demonstrated that RUNX3 can suppress TGF- β 1-induced EMT in esophageal squamous cell carcinoma (ESCC) [47]. In the

present study, expression levels of TGF- β , SMAD molecules and EMT markers such as Snail and Vimentin were increased in *RUNX3* knockdown parental cells. These data support that RUNX3 can regulate EMT through TGF- β /SMAD pathway.

In summary, lapatinib-resistant cell lines were established from SK-BR-3 HER2-amplified breast cancer cells. This study demonstrated that down-regulation of RUNX3 could induce EMT by activating TGF- β /SMAD signal transduction. This is the first study that examined the function of RUNX3 to suppress EMT that was lost during acquired resistance to lapatinib.

**PART II. Replication stress activates DNA
damage response and contributes to
lapatinib resistance in SK-BR-3 cells**

RESULTS

1. Replication stress is elevated by high speed of fork progression in LR cells

In lapatinib-resistant (LR) cells, G1/S phase transition was increased by upregulation of cyclin D1 [48]. Consistent with this finding, early and late S phase populations were increased approximately 2-fold in LR cells (Fig 8A). Next, DNA fiber assay was conducted to examine the cause of increase in S phase. As a result, fork speed was accelerated in LR cells (Fig. 8B). A previous study has reported that high speed of replication fork can induce DNA replication stress [49]. Therefore, a bidirectional replication fork asymmetry as a characteristic of replication stress was confirmed. The asymmetry of forks was increased from 1.18 to 1.82 in LR cells compared with parental cells (Fig. 8B). Phosphorylation level of RPA, a marker of replication stress, was increased in EdU positive population in LR cells (Fig. 8C). Taken together, these observations indicated that replication stress was elevated in LR cells.

If DNA replication and transcription are carried out in the same DNA template, transcription-replication conflicts (T-R conflicts)

will occur, which can lead to DNA damage. When replication fork progresses fast, DNA polymerase encounters RNA polymerase and confers to T–R conflicts. As replication fork speed was increased in LR cells, it was thought that T–R conflicts were generated in LR cells. To prove this hypothesis, this study investigated DNA:RNA hybrid, a product of T–R conflicts. DNA:RNA hybrid positive cells (S9.6 foci > 3) were significantly increased to 55 % in LR cells and LR clones (Fig 8D). These data suggested that acceleration of replication fork progression can cause replication stress in LR cells.

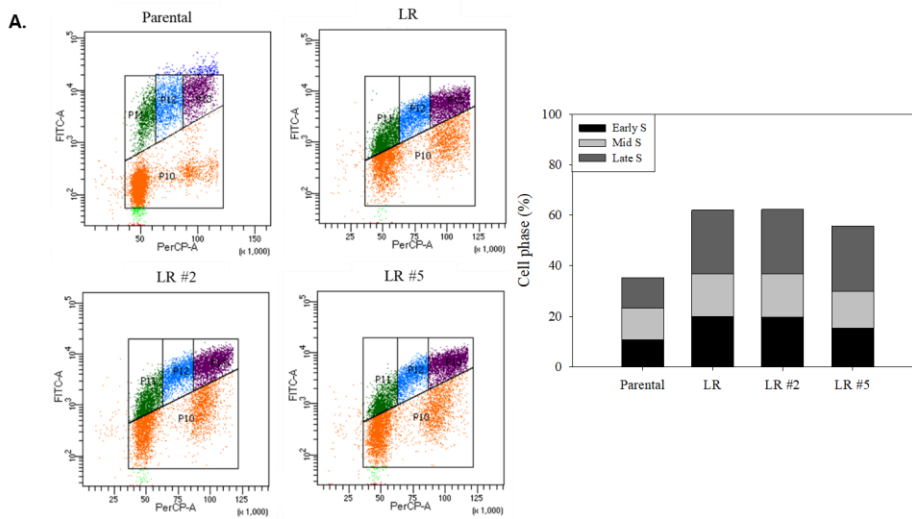


Figure 8. High speed of fork progression in LR cells increases replication stress (A) Cell population of S phase was analyzed by flow cytometry. BrdU incorporation and DNA contents were visualized using anti-BrdU conjugated with FITC and 7-AAD. P11, P12, and P13 are shown, representing early S, mid S, and late S phases, respectively. Bar charts summarize quantification of early S, mid S, and late S phase (%).

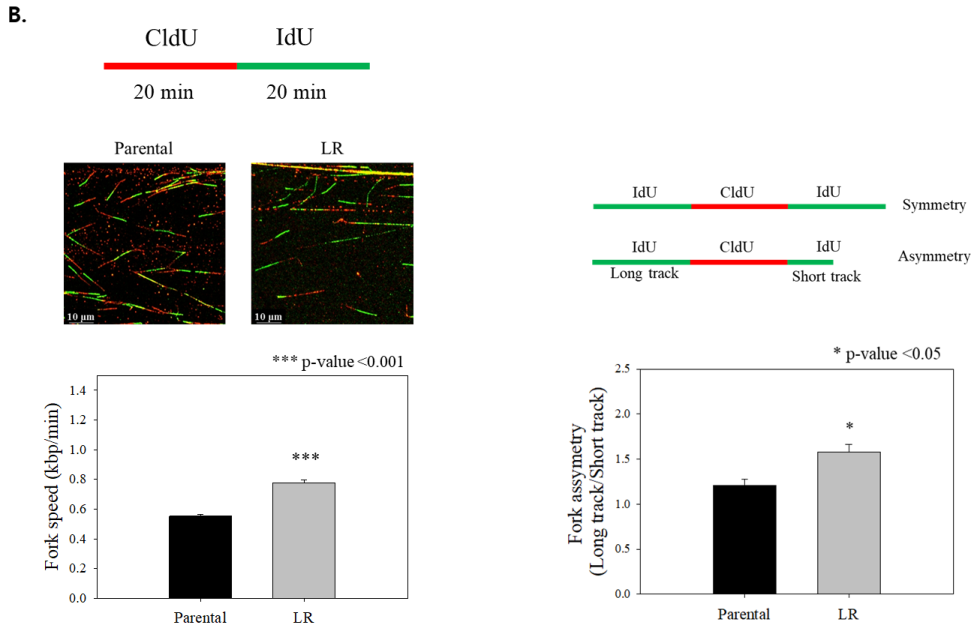


Figure 8. (B) Scheme of DNA fiber assay. Cells were treated sequentially with CldU (red) and IdU (green). Immunofluorescent images represent DNA fibers derived from parental and LR cells. Bar charts summarize quantification of replication velocities and fork asymmetry.

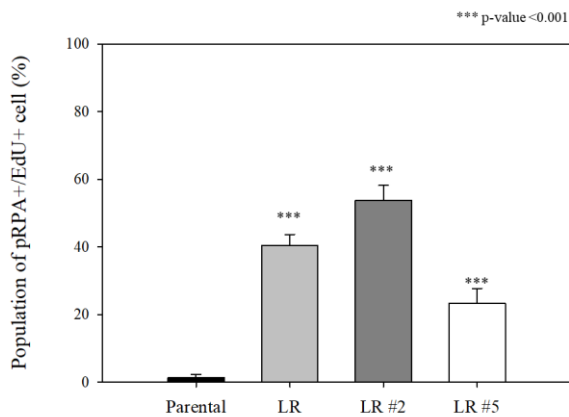
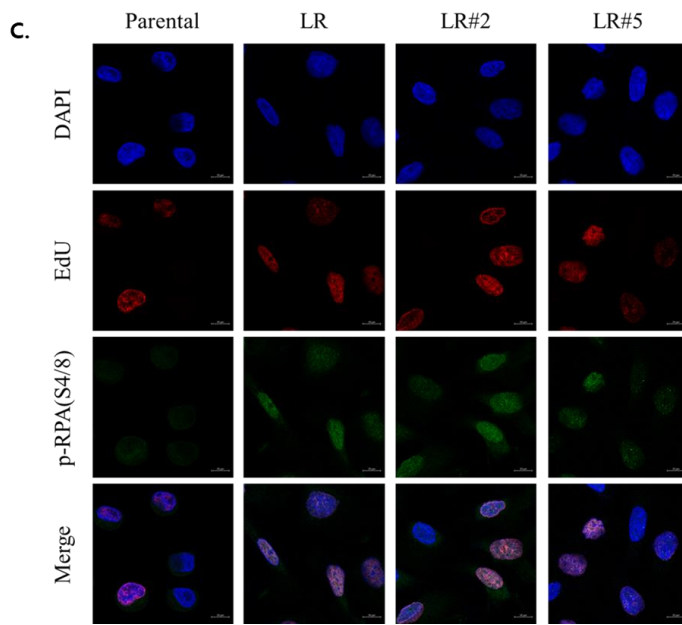


Figure 8. (c) Cells were obtained at 63 X magnification using confocal microscopy. EdU positive cells (red) indicate S phase cells. DNA damage sites were confirmed by p-RPA (S4/8) (green) and nucleus stained with DAPI (blue). Scale bar, 10 μ m. Population of pRPA and EdU positive cells was quantified. Data are presented as mean \pm S.D. (***)p<0.001) of three independent experiments.

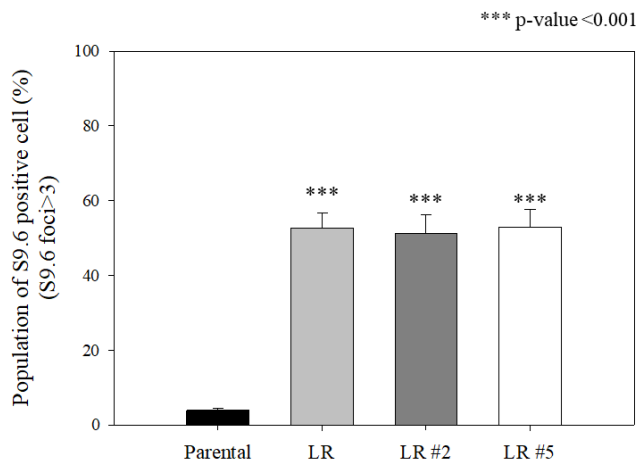
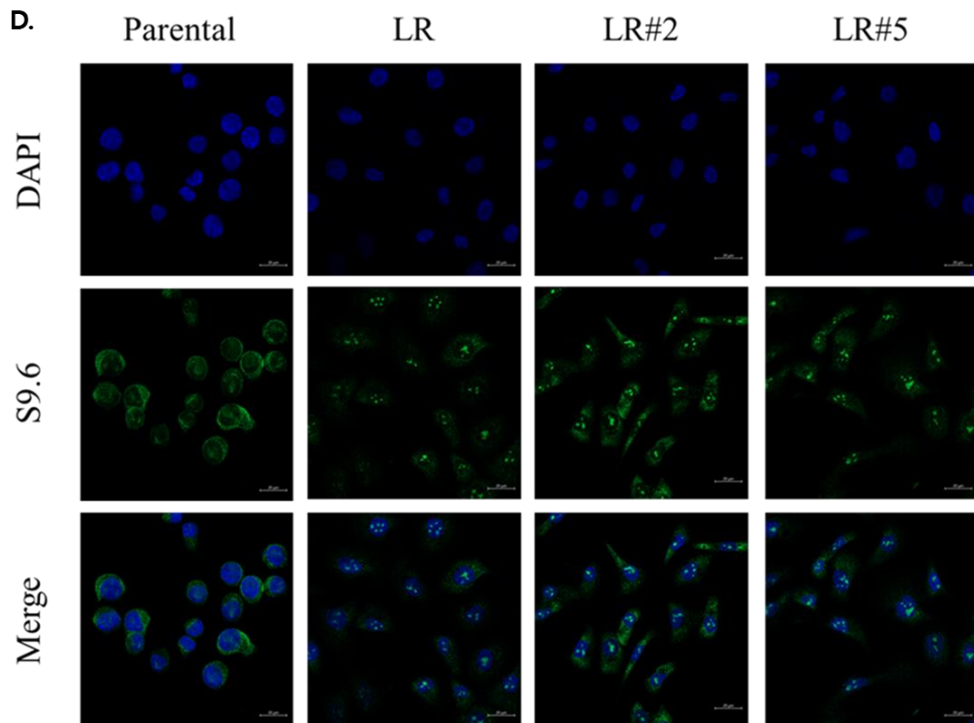


Figure 8. (D) DNA:RNA hybrids were increased in LR cells. S9.6 foci (green) indicate DNA:RNA hybrid with nucleus stained with DAPI (blue). Scale bar, 10 μ m. The bar chart represents the population of S9.6 positive (S9.6 foci > 3) cells (***p<0.001).

2. Cancer stem-like cell (CSC) population shows enhanced replication stress in LR cells

In glioblastoma, replication stress is elevated by T-R conflicts in cancer stem-like cell (CSC) population [50]. As LR cells showed characteristic of CSCs, whether replication stress was enhanced in CSC population of LR cells were examined. In parental cells, the population of EdU-positive cells was more in Sox2-negative population than in Sox2-positive population (20 % vs. 6 %, EdU+/Sox2- vs. EdU+/Sox2+). Contrary to this result, in LR cells, EdU-positive cells were more in Sox2 positive population. This result indicated that CSCs existed in S phase were increased in LR cells (Fig 9A). γ -H2AX, a marker of DNA double-strand breaks, also increased to approximately 40 % in CSCs of LR and LR clones (Fig 9B). S9.6 and Sox2 co-positive cells were significantly increased in LR cells (Fig 9C). Taken together, these results suggest that enhanced replication stress can lead to DNA damage in CSC population of LR cells.

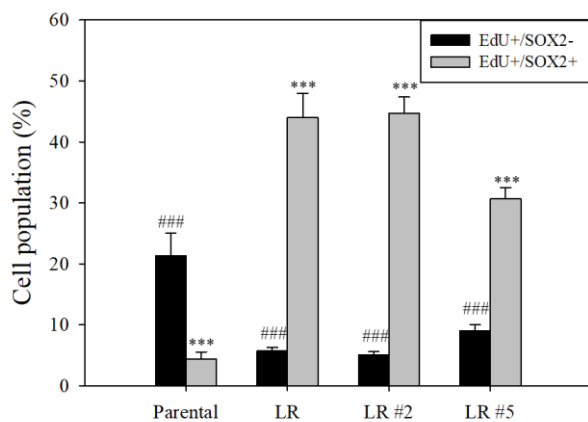
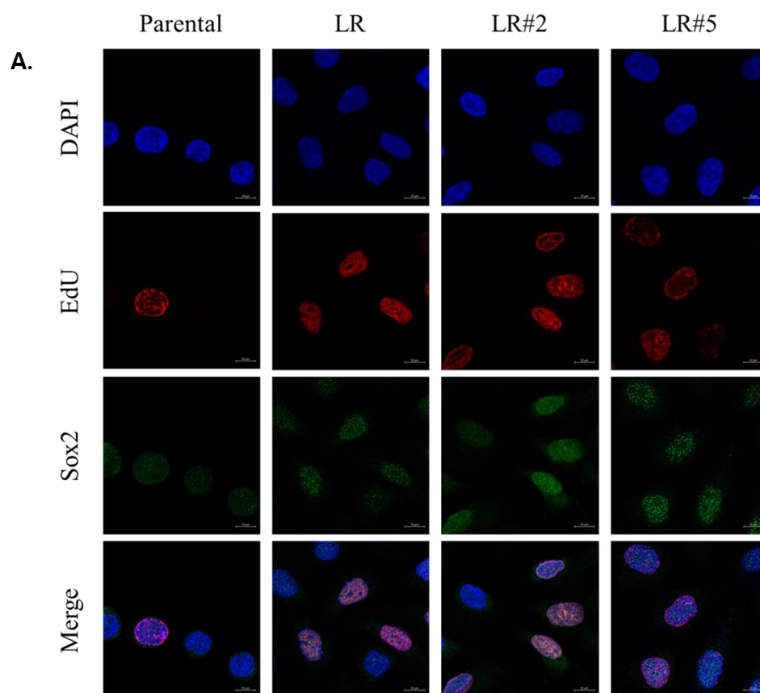


Figure 9. CSC population shows enhanced replication stress in LR cells. (A) EdU, a marker of S phase (red), Sox2, a marker of cancer stem cell (green), and co-positive cells were increased in LR cells. Scale bar, 10 μ m. The bar chart represents cell population (%). (###p-value < 0.001 in EdU+/Sox2-, ***p-value<0.001 in EdU+/Sox2+).

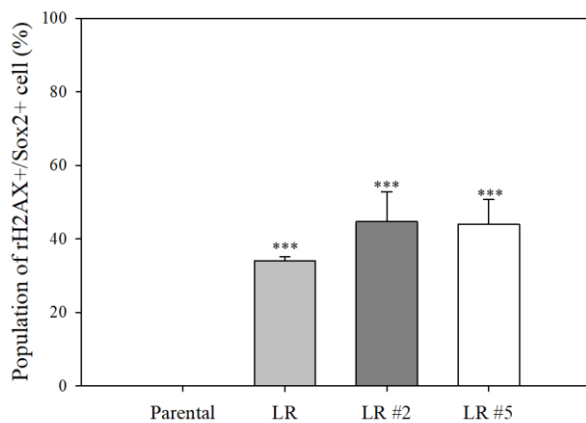
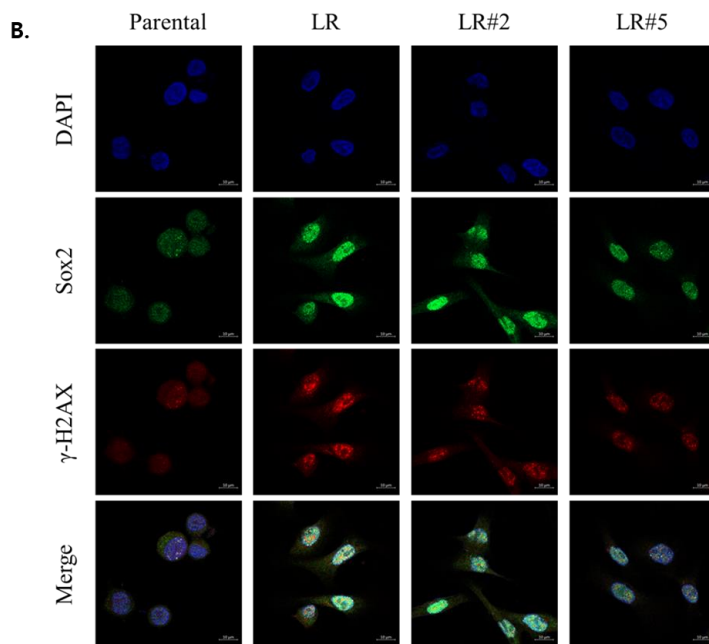


Figure 9. (B) Cells were obtained at 63X magnification using confocal microscopy. DNA double strand breaks (γ -H2AX foci, red) were increased in CSC population of LR cells. Scale bar, 10 μ m. Bar charts summarize quantification of γ -H2AX and Sox2 co-positive cell population (%). 100 cells were counted for each group (***) p-value <0.001).

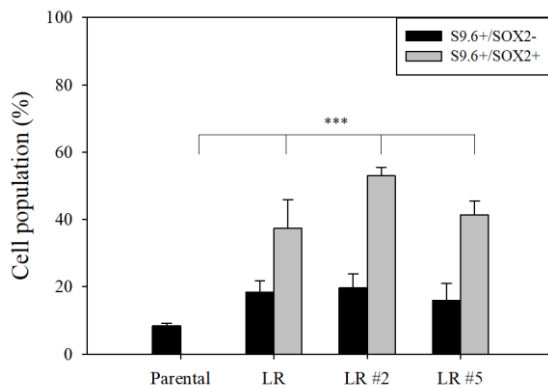
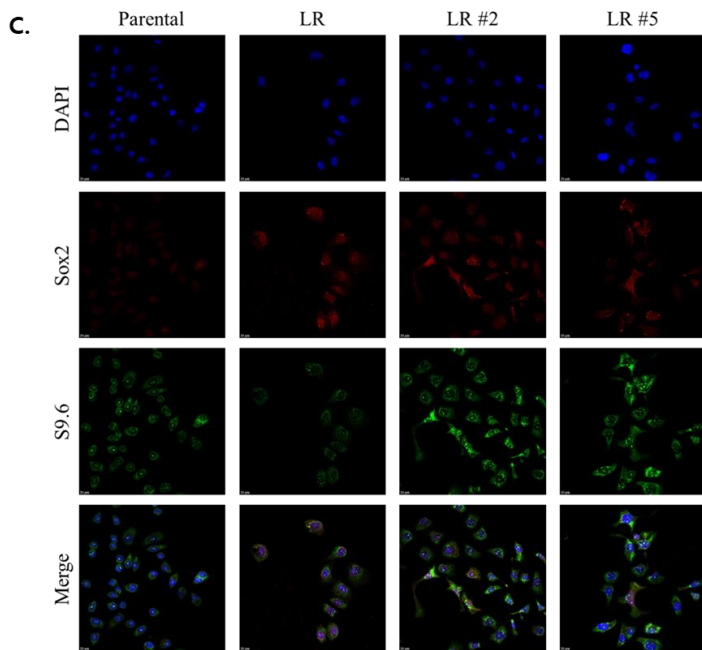


Figure 9. (C) Cells were obtained at 40X magnification using confocal microscopy. DNA:RNA hybrids (S9.6, green) were increased in CSC population (Sox2 positive, red) in LR cells. Scale bar, 20 μ m. Bar charts summarize quantification of S9.6 and Sox2 co-positive cell population (%). 100 cells were counted for each group (***) p-value <0.001).

3. Expression levels of homologous recombination repair (HR) mediated molecules are increased in LR cells

Replication stress is a source of DNA damage response activation. Therefore, it was thought that DNA damage response was activated in LR cells. To determine which DDR mechanism is associated with replication stress in LR cells, transcriptome data were analyzed (Fig. 10A). Transcriptome data showed that homologous recombination repair (HR) mediated factors were upregulated in LR cells (Fig. 10B). Interestingly, expression levels of ATM and ATR were not different between parental and LR cells, although phosphorylation of S296, an auto-phosphorylation sites of Chk1, was increased in LR cells (Fig. 10C). Levels of RAD51, RAD51B, and RAD51C known to be important effectors in HR, were increased in LR cells (Fig. 10D). Activated Chk1 is recruited at DNA damage sites to phosphorylate HR associated molecules [18]. In concordance with this fact, Chk1 and p-RPA (S4/8) were also co-localized in LR cells (Fig. 10E). Taken together, these results showed that expression levels of HR associated molecules were

increased in LR cells and suggested the possibility of enhanced DNA damage repair capacity in LR cells.

A.

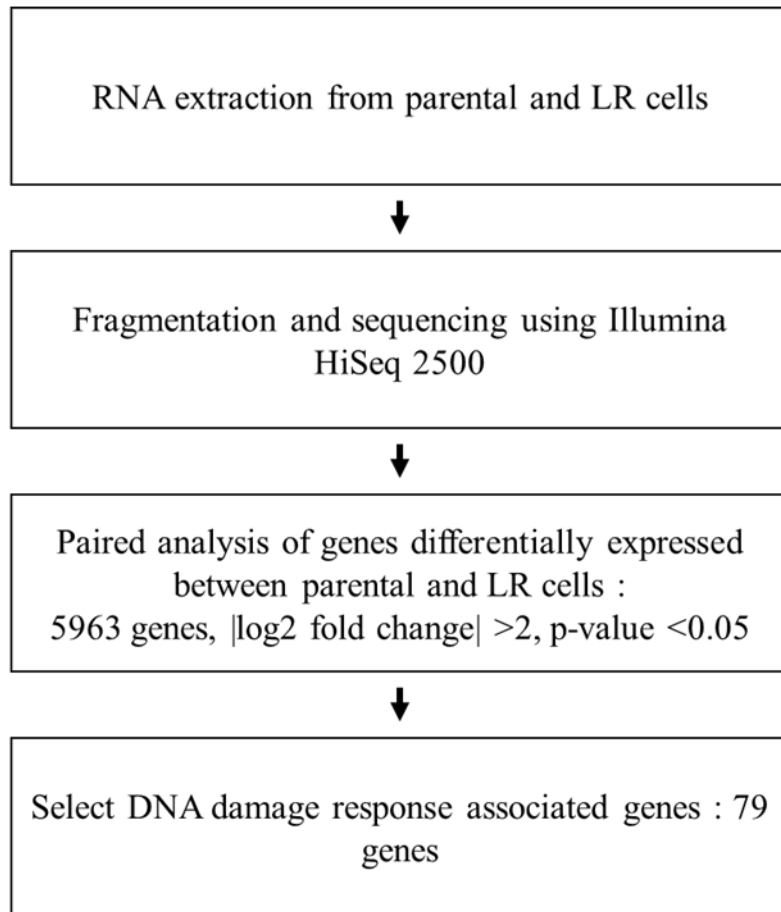


Figure 10. Expression levels of homologous recombination repair (HR) mediated molecules are increased in LR cells (A) Transcriptome analysis performed according to the flow chart.

B.

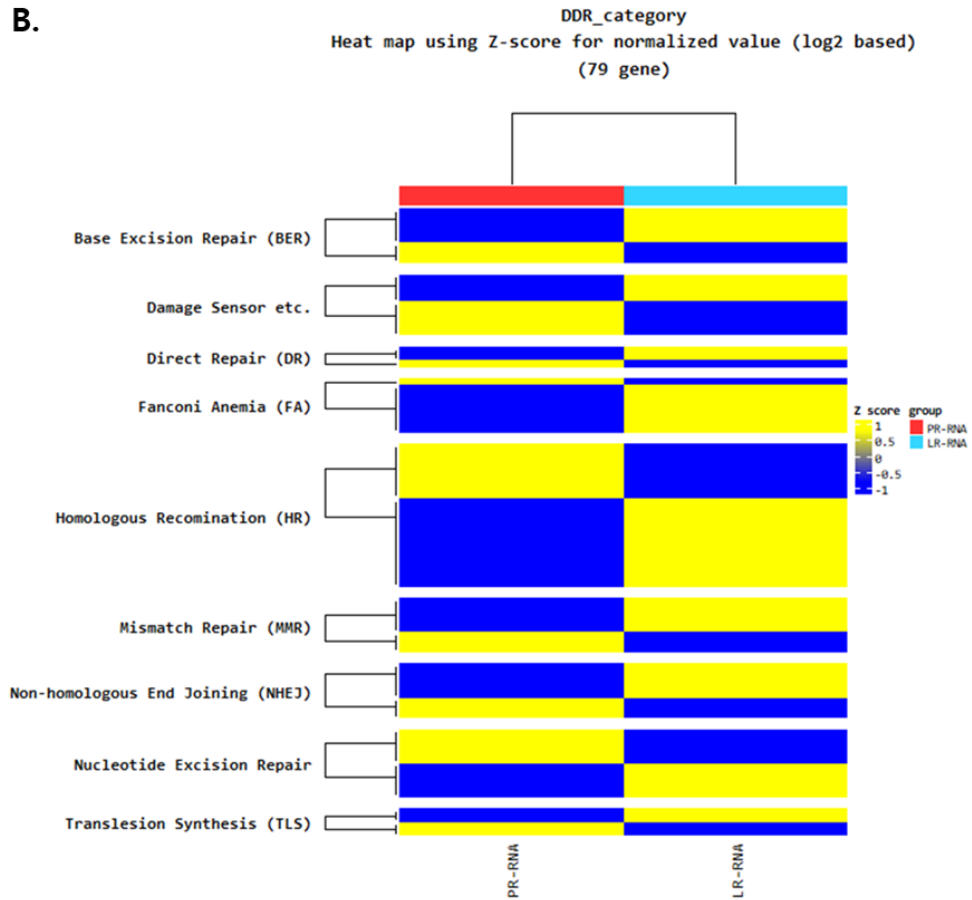


Figure 10. (B) Expression of DNA damage response pathway core molecules were analyzed by RNA sequencing. Homologous recombination repair (HR) associated molecules were increased in LR cells.

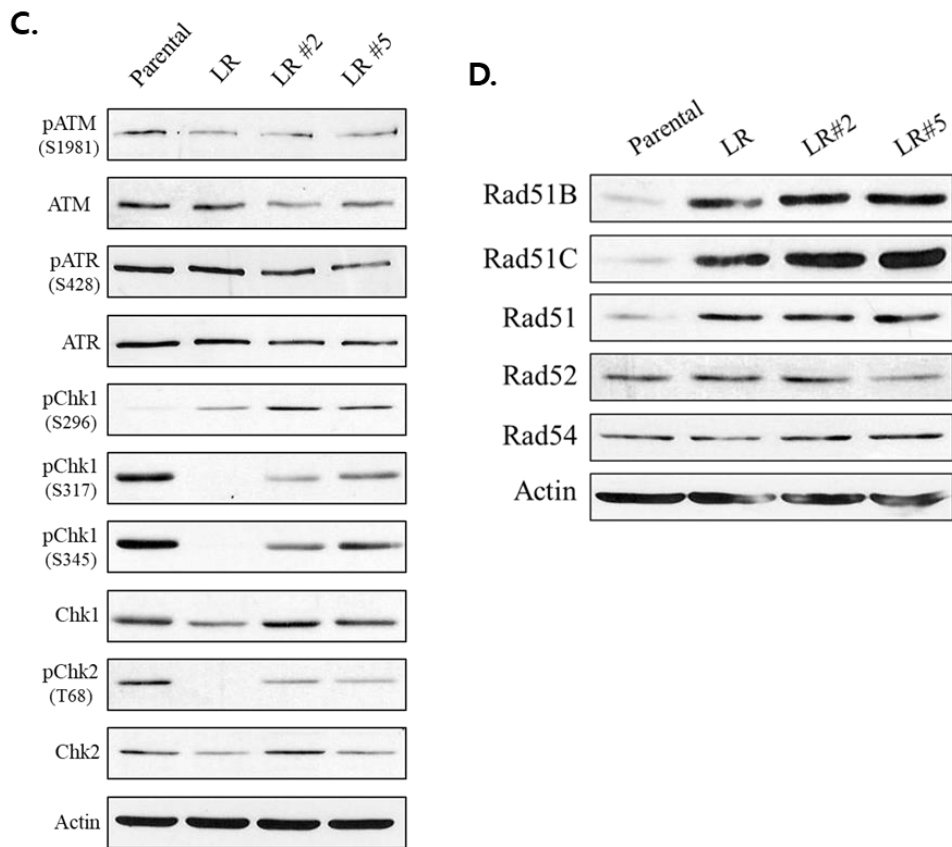


Figure 10. Protein expression levels of (C) ATR–Chk1, ATM–Chk2 pathway and (D) RAD51 paralogs were detected by western blotting. Actin was used as a loading control.

E.

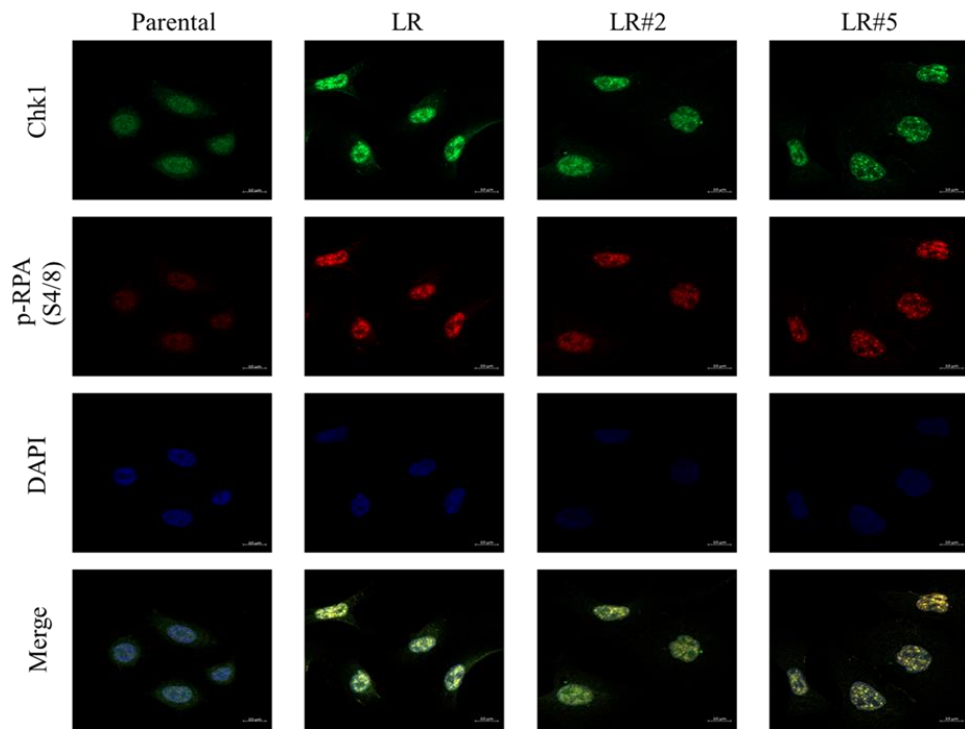


Figure 10. (E) Chk1 is localized at DNA damage sites in LR cells.

4. DNA damage repair capacity is enhanced in LR cells

To confirm DNA damage repair capacity, replication stress and DNA double strand breaks were induced by AZD6738 and irradiation, respectively. After irradiation, phosphorylation of Chk1 was induced in both parental cells and LR cells (Fig. 11A, lane 2). However, phosphorylation of Chk1 was maintained longer in LR cells. Moreover, γ -H2AX was continuously increased in parental cells, whereas enhanced γ -H2AX level was decreased consequently in LR cells (Fig 11A). Consistent with these data, tail of comet disappeared at early time point (Release 1) in LR cells compared with parental cells. The head size of the comet was completely recovered in LR cells, but not in parental cells (Fig. 11B). Replication stress was induced by AZD6738 phosphorylated Chk1 only in LR cells and enhanced γ -H2AX was decreased to a control level. In parental cells, enhanced γ -H2AX was maintained continuously despite activation of Chk2 (Fig. 11C). Comet assay results showed that DNA damages caused by replication stress were recovered completely in LR cells but not in parental cells (Fig.

11D). These results demonstrated that DDR was activated and DNA damage repair capacity was enhanced in LR cells.

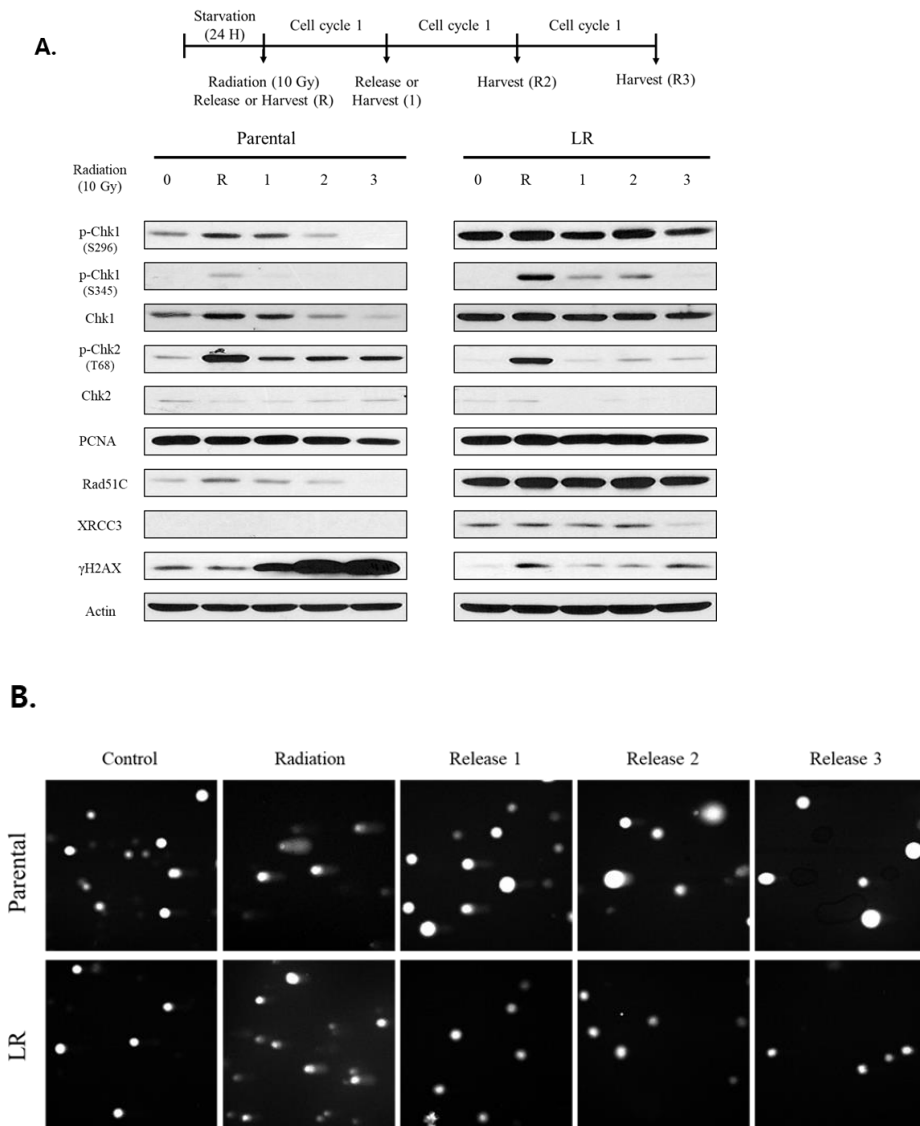


Figure 11. DNA damage repair capacity is enhanced in LR cells. DNA double strand breaks were induced by 10 Gy radiation and cells were released at indicated time points. (A) DNA double strand breaks and DNA damage repair molecules were confirmed by western blotting. (B) DNA breaks and repair capacity were examined by comet assay.

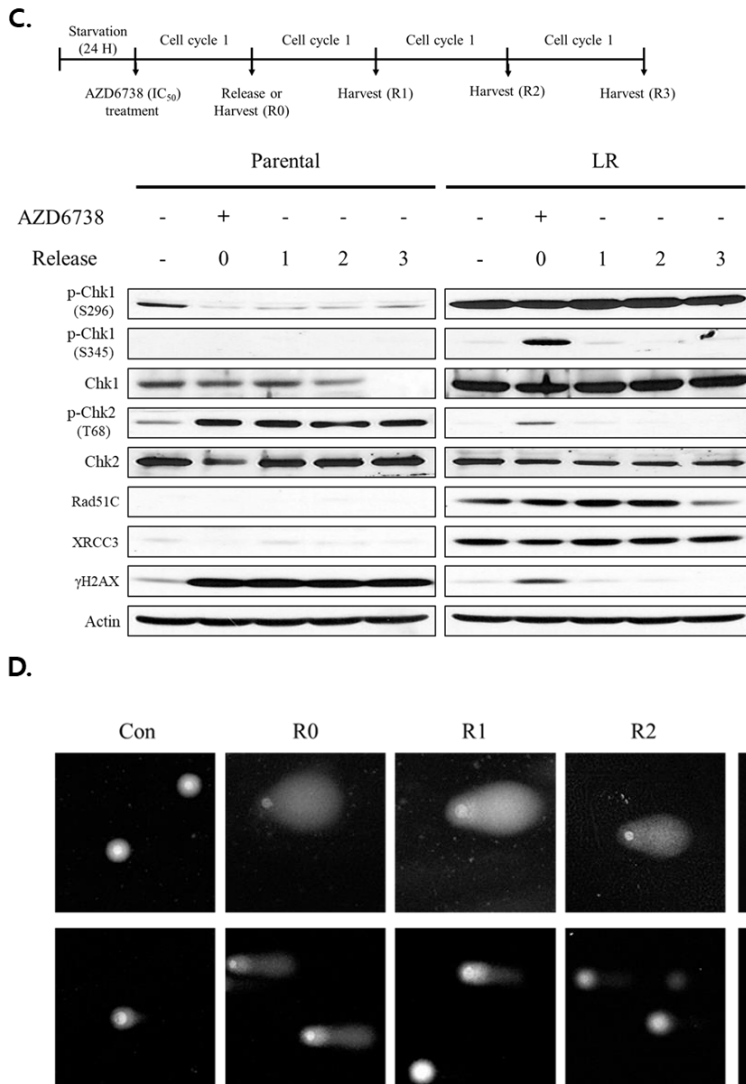


Figure 11. Replication stress was induced by AZD6738 and cells were released at indicated time points. (C) DNA double strand breaks and DNA damage repair molecules were confirmed by western blotting. (D) DNA breaks and repair capacity were examined by comet assay.

5. DDR activation induced replication stress affects lapatinib sensitivity

Activation of DDR is one of the well know mechanisms of chemotherapy or radiation therapy resistance. Recently, studies have suggested that DDR is associated with resistance to trastuzumab [30, 32, 50]. Thus, whether activation of DDR could affect lapatinib sensitivity was determined. To confirm this hypothesis, parental cells were treated with aphidicolin. Since high concentration of aphidicolin induced cell cycle arrest [50, 51], parental cells were treated with low concentrations of aphidicolin and cell cycle was analyzed. It was found that 0.01 $\mu\text{mol/L}$ aphidicolin did not affect cell cycle progression, although it induced replication stress and Chk1 activation. (Fig. 12A and 12B). Therefore, parental cells were cultured with 0.01 $\mu\text{mol/L}$ for further study. The cytotoxicity of lapatinib was decreased in parental cells after exposure to a low concentration of apidicolin (Fig. 12C). These results indicate that DDR induced by replication stress might contribute to resistance to lapatinib. To confirm this hypothesis, HER2 overexpressed MDA-MB-453 cells were treated with a low concentration of aphidicolin and cell viability was

analyzed using MTT assay. Aphidicolin activated Chk1 with induction of replication stress without affecting cell cycle progression. It also attenuated the cytotoxicity of lapatinib in MDA-MB-453 (Fig. 12D, 12E, and 12F). Taken together, these results suggest that replication stress contributes to lapatinib-resistance through DDR activation (Fig. 12G).

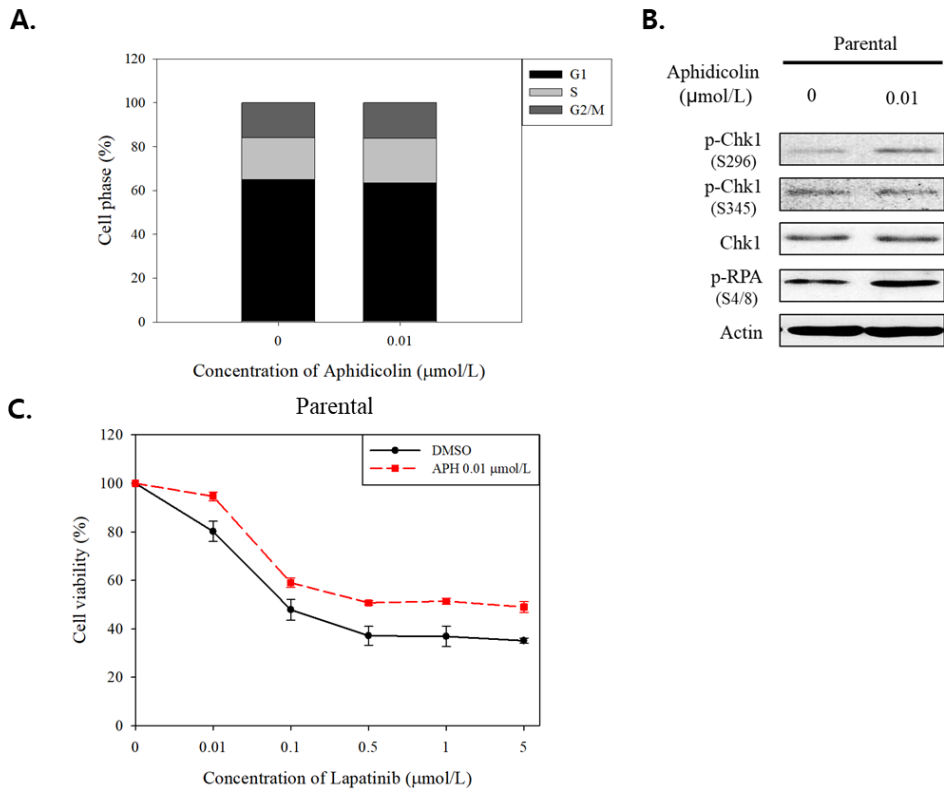


Figure 12. DDR activation induced replication stress affects lapatinib sensitivity. Cells were treated with 0.01 $\mu\text{mol/L}$ aphidicolin for 72 h. (A) Cell cycle was analyzed using DNA contents stained with PI. (B) p-RPA (S4/8), a marker of replication stress, and Chk1 expression were determined by western blotting. (C) Cytotoxicity of lapatinib was measured by MTT assay. Parental cells and LR cells were treated with lapatinib at indicated concentrations. After 72 h, cell viability was measured.

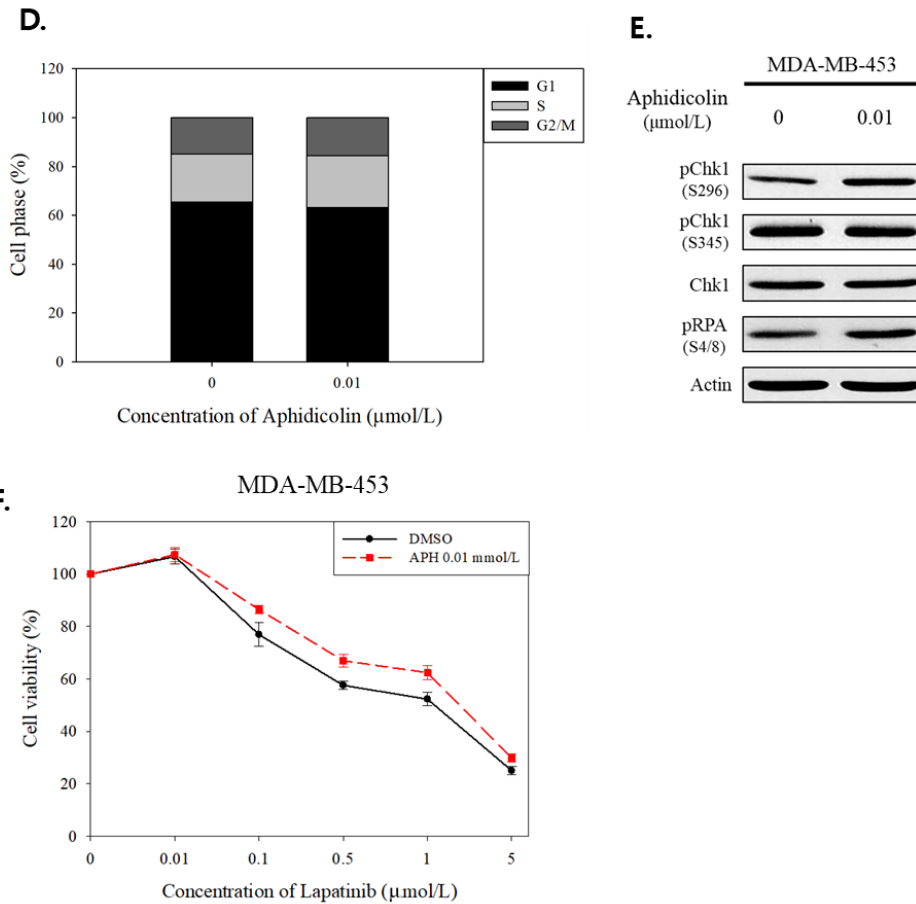


Figure 12. DDR activation induced replication stress affects lapatinib sensitivity. Cells were treated with 0.01 μ mol/L aphidicolin for 72 h. (A) Cell cycle was not affected by aphidicolin. (B) Replication stress and auto-phosphorylation of Chk1 were increased in MDA-MB-453 after treatment with aphidicolin. (C) Cytotoxicity of lapatinib was attenuated after exposure to aphidicolin.

G.

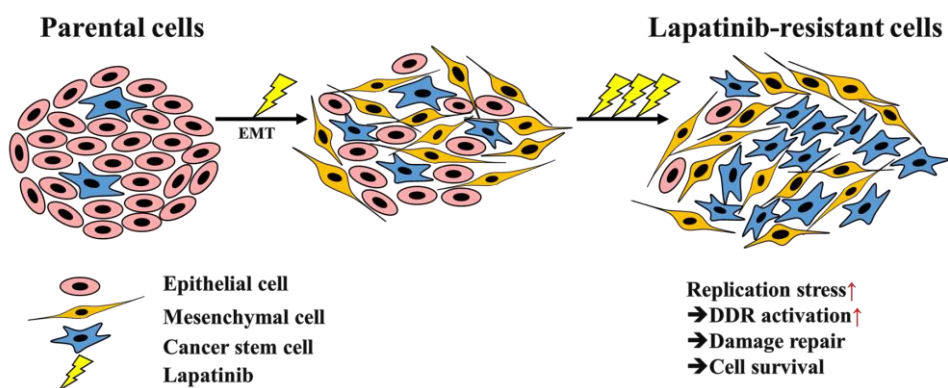


Figure 12. (G) A proposal model for acquired resistance to lapatinib via DDR activation by replication stress. In parental cells, some cancer stem cells existed with epithelial cells. During treatment with lapatinib, parental cells transformed to EMT phenotype and cancer stem cell population increased. After continuous lapatinib exposure, major population of LR cells transformed to mesenchymal cells or cancer stem cells. In these cells, elevated replication stress activates DDR and contributes to resistance to lapatinib.

DISCUSSION

Although lapatinib improves progression free survival (PFS) in HER2–amplified breast cancer patients, acquired resistance remains a challenge. Understanding the mechanism of resistance to lapatinib is crucial to overcome the resistance problem and to establish novel therapeutic strategies.

Various studies have suggested that persistent activation of HER2 downstream such as PI3K–AKT and MAPK pathways can lead to lapatinib resistance [6]. However, a previous study has shown that activities of these pathways are reduced in LR cells [35]. Thus, the present study explored novel mechanism involved in lapatinib resistance.

According to a recent study, a decrease of G1 phase can induce replication stress and reduce fork speed in mouse embryonic stem cells [51]. In LR cells, G1 phase was decreased as G1/S transition accelerated, but replication fork speed was increased. Originally, replication stress was defined as a replication fork slow down or fork stalling. However, a recent study has suggested that it is an aberrant acceleration of replication fork speed by PARP inhibitor that causes DNA damage without fork stalling. This phenomenon is considered as a replication stress [49]. An acceleration of fork progression can increase the chance of an encounter between DNA

and RNA polymerase, eventually leading to T–R conflicts [52]. LR cells showed markedly increased DNA damage and S9.6 foci, a marker of T–R conflicts. These data indicate that acceleration of fork speed can cause replication stress in LR cells.

Chk1 is an important mediator of DDR. It has a crucial role in regulation of cell cycle progression. When DNA damage occurs, Chk1 is phosphorylated at multiple sites. Ser317 and Ser345 are phosphorylated dependent on ATR and Ser296 is auto-phosphorylated [53]. A previous study has shown that phosphorylation of Chk1 ser345 is increased in cells that are less sensitive to lapatinib and that overexpression of Chk1 can attenuate lapatinib sensitivity in HER2–positive gastric cancer cells [31]. Contrary to this, phosphorylation of Chk1 ser345 was decreased, whereas auto-phosphorylation of ser296 was significantly increased in LR cells. Several studies have demonstrated that Chk1 phosphorylation sites affect Chk1 localization [53, 54]. Unfortunately difference of function depends on phosphorylation sites remains unknown. Therefore, understanding Chk1 phosphorylation sites might provide insights for understanding the mechanism of resistance.

CSCs can tolerate endogenous and exogenous stress through robust DDR. This property often increases the dependency of CSCs

on a specific DDR pathway. Therefore, CSCs can be vulnerable to DDR targeted drugs [55]. Because Chk1 activation was observed in LR cells, ATR–Chk1 pathway was inhibited with an ATR inhibitor in this study. Auto–phosphorylation of Chk1 was significantly decreased. However, cytotoxicity was not observed in LR cells (Data not shown).

RAD51 is a key molecule in homologous recombination repair and replication fork restart [27]. RAD51 and RAD51 paralogs were increased in LR cells. Recent studies have suggested that RAD51 inhibitor does not affect replication fork progression in normal condition, but reduces fork progression in colorectal cancer cells in the presence of a mild replication stress [21]. Therefore, understanding the antitumor effect of RAD51 inhibitor might help us develop a novel therapeutic strategy for lapatinib resistant patients.

In summary, replication stress was elevated by acceleration of replication fork progression in CSC population of LR cells. Enhanced replication stress activated DDR and attenuated lapatinib sensitivity. These results could help us understand the association of lapatinib resistance with DDR.

References

1. Sung H., J. Ferlay, R.L. Siegel, M. Laversanne, I. Soerjomataram, A. Jemal, et al., *Global Cancer Statistics 2020: GLOBOCAN Estimates of Incidence and Mortality Worldwide for 36 Cancers in 185 Countries*. CA Cancer J Clin, 2021. **71**(3): p. 209–249.
2. Kang S.Y., S.B. Lee, Y.S. Kim, Z. Kim, H.Y. Kim, H.J. Kim, et al., *Breast Cancer Statistics in Korea, 2018*. J Breast Cancer, 2021. **24**(2): p. 123–137.
3. Chen L M.B., Jathal MK, Madhav A, Johnson SD, van Spyk E, Mikhailova M, et al., *Dual EGFR/HER2 inhibition sensitizes prostate cancer cells to androgen withdrawal by suppressing ErbB3*. Clin Cancer Res, 2011.
4. Valentina D'Amato L.R., Luigi Formisano, Mario Giuliano, Sabino De Placido, Roberta Rosa , Roberto Bianco *Mechanisms of lapatinib resistance in HER2-driven breast cancer*. Cancer Treat Rev, 2015.
5. Xia W., S. Bacus, P. Hegde, I. Husain, J. Strum, L. Liu, et al., *A model of acquired autoresistance to a potent ErbB2 tyrosine kinase inhibitor and a therapeutic strategy to prevent its onset in breast cancer*. Proc Natl Acad Sci U S A, 2006. **103**(20): p. 7795–800.
6. D'Amato V., L. Raimondo, L. Formisano, M. Giuliano, S. De Placido, R. Rosa, et al., *Mechanisms of lapatinib resistance in HER2-driven breast cancer*. Cancer Treat Rev, 2015. **41**(10): p. 877–83.
7. Nahta R., L.X. Yuan, Y. Du, and F.J. Esteva, *Lapatinib induces apoptosis in trastuzumab-resistant breast cancer cells: effects on insulin-like growth factor I signaling*. Mol Cancer Ther, 2007. **6**(2): p. 667–74.
8. Geyer C.E., J. Forster, D. Lindquist, S. Chan, C.G. Romieu, T. Pienkowski, et al., *Lapatinib plus capecitabine for HER2-positive advanced breast cancer*. N Engl J Med, 2006. **355**(26): p. 2733–43.
9. Kim H.P., S.W. Han, S.H. Song, E.G. Jeong, M.Y. Lee, D. Hwang, et al., *Testican-1-mediated epithelial-mesenchymal transition signaling confers acquired resistance to lapatinib in HER2-positive gastric cancer*. Oncogene, 2014. **33**(25): p. 3334–41.
10. Burnett J.P., H. Korkaya, M.D. Ouzounova, H. Jiang, S.J. Conley, B.W. Newman, et al., *Trastuzumab resistance induces EMT to transform HER2(+) PTEN(-) to a triple negative breast cancer that requires unique treatment options*. Sci Rep, 2015. **5**: p. 15821.
11. Hua W., P. Ten Dijke, S. Kostidis, M. Giera, and M. Hornsveid, *TGFbeta-induced metabolic reprogramming during epithelial-to-mesenchymal transition in cancer*. Cell Mol Life Sci, 2019.
12. Lu W. and Y. Kang, *Epithelial-Mesenchymal Plasticity in Cancer Progression and Metastasis*. Dev Cell, 2019. **49**(3): p. 361–374.
13. Katsuno Y., D.S. Meyer, Z. Zhang, K.M. Shokat, R.J. Akhurst, K. Miyazono, et al., *Chronic TGF-beta exposure drives stabilized EMT, tumor stemness, and cancer drug resistance with vulnerability to bitopic mTOR inhibition*. Sci Signal, 2019. **12**(570).

14. Bai J., H.M. Yong, F.F. Chen, W.B. Song, C. Li, H. Liu, et al., *RUNX3 is a prognostic marker and potential therapeutic target in human breast cancer*. J Cancer Res Clin Oncol, 2013. **139**(11): p. 1813–23.
15. Huang B., Z. Qu, C.W. Ong, Y.H. Tsang, G. Xiao, D. Shapiro, et al., *RUNX3 acts as a tumor suppressor in breast cancer by targeting estrogen receptor alpha*. Oncogene, 2012. **31**(4): p. 527–34.
16. Ito Y. and K. Miyazono, *RUNX transcription factors as key targets of TGF-beta superfamily signaling*. Curr Opin Genet Dev, 2003. **13**(1): p. 43–7.
17. Zaidi S.K., A.J. Sullivan, A.J. van Wijnen, J.L. Stein, G.S. Stein, and J.B. Lian, *Integration of Runx and Smad regulatory signals at transcriptionally active subnuclear sites*. Proc Natl Acad Sci U S A, 2002. **99**(12): p. 8048–53.
18. Yang H., J. Fu, L. Yao, A. Hou, and X. Xue, *Runx3 is a key modulator during the epithelial-mesenchymal transition of alveolar type II cells in animal models of BPD*. Int J Mol Med, 2017. **40**(5): p. 1466–1476.
19. Voon D.C., H. Wang, J.K. Koo, T.A. Nguyen, Y.T. Hor, Y.S. Chu, et al., *Runx3 protects gastric epithelial cells against epithelial-mesenchymal transition-induced cellular plasticity and tumorigenicity*. Stem Cells, 2012. **30**(10): p. 2088–99.
20. Halazonetis T.D., V.G. Gorgoulis and J. Bartek, *An oncogene-induced DNA damage model for cancer development*. Science, 2008. **319**(5868): p. 1352–5.
21. Feu S., F. Unzueta, A. Ercilla, A. Perez-Venteo, M. Jaumot, and N. Agell, *RAD51 is a druggable target that sustains replication fork progression upon DNA replication stress*. PLoS One, 2022. **17**(8): p. e0266645.
22. Guerrero Llobet S., B. van der Vegt, E. Jongeneel, R.D. Bense, M.C. Zwager, C.P. Schroder, et al., *Cyclin E expression is associated with high levels of replication stress in triple-negative breast cancer*. NPJ Breast Cancer, 2020. **6**: p. 40.
23. Murayama T., Y. Takeuchi, K. Yamawaki, T. Natsume, M. Li, R.N. Marcela, et al., *MCM10 compensates for Myc-induced DNA replication stress in breast cancer stem-like cells*. Cancer Sci, 2021. **112**(3): p. 1209–1224.
24. Segeren H.A. and B. Westendorp, *Mechanisms used by cancer cells to tolerate drug-induced replication stress*. Cancer Lett, 2022. **544**: p. 215804.
25. Buisson R., J.L. Boisvert, C.H. Benes, and L. Zou, *Distinct but Concerted Roles of ATR, DNA-PK, and Chk1 in Countering Replication Stress during S Phase*. Mol Cell, 2015. **59**(6): p. 1011–24.
26. Wassing I.E., E. Graham, X. Saayman, L. Rampazzo, C. Ralf, A. Bassett, et al., *The RAD51 recombinase protects mitotic chromatin in human cells*. Nat Commun, 2021. **12**(1): p. 5380.
27. Berti M., F. Teloni, S. Mijic, S. Ursich, J. Fuchs, M.D. Palumbieri, et al., *Sequential role of RAD51 paralog complexes in replication fork remodeling and restart*. Nat Commun, 2020. **11**(1): p. 3531.
28. Morgan M.A. and T.S. Lawrence, *Molecular Pathways: Overcoming*

- Radiation Resistance by Targeting DNA Damage Response Pathways.* Clin Cancer Res, 2015. **21**(13): p. 2898–904.
29. Li L.Y., Y.D. Guan, X.S. Chen, J.M. Yang, and Y. Cheng, *DNA Repair Pathways in Cancer Therapy and Resistance.* Front Pharmacol, 2020. **11**: p. 629266.
 30. Oh K.S., A.R. Nam, J.H. Bang, H.R. Seo, J.M. Kim, J. Yoon, et al., *A synthetic lethal strategy using PARP and ATM inhibition for overcoming trastuzumab resistance in HER2-positive cancers.* Oncogene, 2022. **41**(32): p. 3939–3952.
 31. Bai M., N. Song, X. Che, X. Wang, X. Qu, and Y. Liu, *Chk1 activation attenuates sensitivity of lapatinib in HER2-positive gastric cancer.* Cell Biol Int, 2018. **42**(7): p. 781–793.
 32. Lubennikova E., L. Zhukova, M. Lichinitser, E. Stepanova, Y. Vishnevskaya, D. Khochenkov, et al., *ERCC1 and XRCC1 as prognostic biomarkers for early HER2-positive breast cancer.* Journal of Clinical Oncology, 2018. **36**(15_suppl): p. e12562–e12562.
 33. Fabregat A., K. Sidiropoulos, G. Viteri, O. Forner, P. Marin-Garcia, V. Arnau, et al., *Reactome pathway analysis: a high-performance in-memory approach.* BMC Bioinformatics, 2017. **18**(1): p. 142.
 34. Zhao M., Y. Liu, C. Zheng, and H. Qu, *dbEMT 2.0: An updated database for epithelial-mesenchymal transition genes with experimentally verified information and precalculated regulation information for cancer metastasis.* J Genet Genomics, 2019. **46**(12): p. 595–597.
 35. Kim S.H., A. Min, S. Kim, D.H. Ha, H. Jang, Y.J. Kim, et al., *Abstract 4116: Acquired lapatinib resistant induces EMT-phenotype in breast cancer cells via Src and RUNX3.* Cancer Research, 2017. **77**(13_Supplement): p. 4116–4116.
 36. Jiang Y., D. Tong, G. Lou, Y. Zhang, and J. Geng, *Expression of RUNX3 gene, methylation status and clinicopathological significance in breast cancer and breast cancer cell lines.* Pathobiology, 2008. **75**(4): p. 244–51.
 37. Liu J., X. Chen, T. Ward, Y. Mao, J. Bockhorn, X. Liu, et al., *Niclosamide inhibits epithelial-mesenchymal transition and tumor growth in lapatinib-resistant human epidermal growth factor receptor 2-positive breast cancer.* Int J Biochem Cell Biol, 2016. **71**: p. 12–23.
 38. Patel A., H. Sabbineni, A. Clarke, and P.R. Somanath, *Novel roles of Src in cancer cell epithelial-to-mesenchymal transition, vascular permeability, microinvasion and metastasis.* Life Sci, 2016. **157**: p. 52–61.
 39. Formisano L., L. Nappi, R. Rosa, R. Marciano, C. D'Amato, V. D'Amato, et al., *Epidermal growth factor-receptor activation modulates Src-dependent resistance to lapatinib in breast cancer models.* Breast Cancer Res, 2014. **16**(3): p. R45.
 40. Galle E., B. Thienpont, S. Cappuyns, T. Venken, P. Busschaert, M. Van Haele, et al., *DNA methylation-driven EMT is a common mechanism of resistance to various therapeutic agents in cancer.*

- Clin Epigenetics, 2020. **12**(1): p. 27.
41. Chen C.C., K.D. Lee, M.Y. Pai, P.Y. Chu, C.C. Hsu, C.C. Chiu, et al., *Changes in DNA methylation are associated with the development of drug resistance in cervical cancer cells*. Cancer Cell Int, 2015. **15**: p. 98.
 42. Liu Z., L. Chen, X. Zhang, X. Xu, H. Xing, Y. Zhang, et al., *RUNX3 regulates vimentin expression via miR-30a during epithelial-mesenchymal transition in gastric cancer cells*. J Cell Mol Med, 2014. **18**(4): p. 610-23.
 43. Kataoka J., H. Shiraha, S. Horiguchi, H. Sawahara, D. Uchida, T. Nagahara, et al., *Loss of Runt-related transcription factor 3 induces resistance to 5-fluorouracil and cisplatin in hepatocellular carcinoma*. Oncol Rep, 2016. **35**(5): p. 2576-82.
 44. Horiguchi S., H. Shiraha, T. Nagahara, J. Kataoka, M. Iwamuro, M. Matsubara, et al., *Loss of runt-related transcription factor 3 induces gemcitabine resistance in pancreatic cancer*. Mol Oncol, 2013. **7**(4): p. 840-9.
 45. Kretschmar M., *Transforming growth factor-beta and breast cancer: Transforming growth factor-beta/SMAD signaling defects and cancer*. Breast Cancer Res, 2000. **2**(2): p. 107-15.
 46. Huang F., Q. Shi, Y. Li, L. Xu, C. Xu, F. Chen, et al., *HER2/EGFR-AKT Signaling Switches TGFbeta from Inhibiting Cell Proliferation to Promoting Cell Migration in Breast Cancer*. Cancer Res, 2018. **78**(21): p. 6073-6085.
 47. Xiao Z., Y. Tian, Y. Jia, Q. Shen, W. Jiang, G. Chen, et al., *RUNX3 inhibits the invasion and migration of esophageal squamous cell carcinoma by reversing the epithelialmesenchymal transition through TGFbeta/Smad signaling*. Oncol Rep, 2020. **43**(4): p. 1289-1299.
 48. Jeong D.E., A. Min, S. Kim, S.H. Kim, Y. Park, Y. Yang, et al., *Abstract 3815: Overcoming acquired resistance of Lapatinib in breast cancer with Palbociclib*. Cancer Research, 2019. **79**(13_Supplement): p. 3815-3815.
 49. Maya-Mendoza A., P. Moudry, J.M. Merchut-Maya, M. Lee, R. Strauss, and J. Bartek, *High speed of fork progression induces DNA replication stress and genomic instability*. Nature, 2018. **559**(7713): p. 279-284.
 50. Carruthers R.D., S.U. Ahmed, S. Ramachandran, K. Strathdee, K.M. Kurian, A. Hedley, et al., *Replication Stress Drives Constitutive Activation of the DNA Damage Response and Radioresistance in Glioblastoma Stem-like Cells*. Cancer Res, 2018. **78**(17): p. 5060-5071.
 51. Ahuja A.K., K. Jodkowska, F. Teloni, A.H. Bizard, R. Zellweger, R. Herrador, et al., *A short G1 phase imposes constitutive replication stress and fork remodelling in mouse embryonic stem cells*. Nat Commun, 2016. **7**: p. 10660.
 52. Wu W., J.N. He, M. Lan, P. Zhang, and W.K. Chu, *Transcription-Replication Collisions and Chromosome Fragility*. Front Genet, 2021. **12**: p. 804547.

53. Okita N., S. Minato, E. Ohmi, S. Tanuma, and Y. Higami, *DNA damage-induced CHK1 autophosphorylation at Ser296 is regulated by an intramolecular mechanism*. FEBS Lett, 2012. **586**(22): p. 3974-9.
54. Niida H., Y. Katsuno, B. Banerjee, M.P. Hande, and M. Nakanishi, *Specific role of Chk1 phosphorylations in cell survival and checkpoint activation*. Mol Cell Biol, 2007. **27**(7): p. 2572-81.
55. Manic G., A. Sistigu, F. Corradi, M. Musella, R. De Maria, and I. Vitale, *Replication stress response in cancer stem cells as a target for chemotherapy*. Semin Cancer Biol, 2018. **53**: p. 31-41.

국문 초록

인간 상피 성장인자 수용체 2 (HER2) 는 HER2 양성 유방암 환자에서 중요한 치료 표적이다. EGFR과 HER2를 표적으로 한 lapatinib은 효과적인 tyrosine kinase 억제제로, HER2 양성 전이성 유방암 환자 치료제이나, 일정기간 사용한 후에는 내성이 발생하므로 lapatinib에 대한 내성 기전에 대한 연구가 필요하다.

본 연구에서는 lapatinib 내성 SK-BR-3세포주 (LR)를 수립하고 lapatinib 내성을 이해하기 위해 LR세포주의 특성을 분석하였다. LR세포주에서 암 줄기세포 마커와 세포의 이동성과 침윤능을 증가시키는 TGF- β 신호전달에 관여하는 단백질들의 발현과 함께 epithelial-to-mesenchymal transition (EMT) 현상이 확인되었다. 반면에 EMT에 관여하는 단백질의 발현을 조절하여 세포 이동과 침윤을 조절하는 암 억제 유전자로 알려진 전사인자 *RUNX3*의 발현은 LR 세포주에서 감소하였다.

다음으로, LR 세포주에서 복제 스트레스가 증가한 것을 관찰하였다. LR 세포주에서 DNA 손상 복구 관련 단백질들의 발현이 증가함으로써 인해 DNA 손상 복구능이 증가하였음을 확인하였다. HER2 양성 유방암세포에서 복제 스트레스가 DNA 손상 반응 신호전달을 활성화하고 lapatinib에 대한 세포독성을 약화시키는 것을 확인하였다. 이러한 결과들을 통해서 복제 스트레스에 의한 DNA 손상 복구 반응의 활성화가 lapatinib 내성에 기여한다는 것을 확인하였다.

Keywords: HER2, Lapatinib, 내성, EMT, 복제 스트레스, DNA 손상 복구 반응

Student Number: 2017-31271

Acknowledgement

This work was supported by a grant (2020R1A2C3010883) of the National Research Foundation of Korea (NRF) funded by the Korea government (MSIT).